SUPPLEMENT TO AN ANALYTICAL FRAMEWORK TO PRICE LONG-DATED CLIMATE-EXPOSED ASSETS

PAULINE CHIKHANI AND JEAN-PAUL RENNE

ABSTRACT. The supplemental appendix is organized as follows: Section S.A provides the proofs of the Proposition 1, in an extended version of the model where η_t is a vector that follows a Gaussian vector autoregressive model. (The baseline model uses only one Gaussian non-persistent shock, denoted by $\eta_{A,t}$, see eq. 10.) Subsection S.A.2 proves Proposition 2. Subsection S.A.3 presents propositions to compute the conditional means and variances of W_t and X_t. Section S.B provides the proof of the pricing propositions of the paper. Specifically, Subsection S.B.1 provides the proof of Proposition 3, that solves for the value function. Subsection S.B.2 provides the proof of Proposition 4, that solves for the SDF. Subsection S.B.3 provides the proof of Proposition 5, which provides the formula to price a basic payoff. Section S.C details the calibration approach. Section S.D develops a version of the model where Epstein-Zin preferences are replaced with time-separable power-utility preferences. Subsection S.E reports the resulting mitigation path and discusses the assumption according to which agents do not dynamically re-optimize mitigation. Section S.F reports additional results. Subsection S.F.1 discusses the relationship between the SCC risk premium and the temperature risk premium. Subsection S.F.2 documents the sensitivity of long-term rates to key modeling ingredients. Subsection S.F.3 shows how the model can be combined with the Black-Scholes-Merton framework (Black and Scholes, 1973; Merton, 1974) to investigate the influence of climate risks on bond and equity prices.

S.A. STATE VECTOR'S CONDITIONAL MOMENTS AND LAPLACE TRANSFORM

S.A.1. **Laplace transform of the state vector.** This section provides the Laplace transform of the state vector $X_t = [Z_t' W_t']'$, with $Z_t = [\tilde{y}_t \mathcal{E}_t F_t M_{AT,t} M_{UP,t} M_{LO,t} T_{AT,t} T_{LO,t} H_t]'$, and $W_t = [\eta_t' D_t N_t T_{AT,t} \Delta H_t]'$. The formula derived in this appendix is more general than in the main text of the paper, as η_t here is a vector of dimension $n_\eta \times 1$; this vector follows a Gaussian vector auto-regressive process:

$$\eta_t = \Phi \eta_{t-1} + \varepsilon_{\eta,t}, \quad \varepsilon_{\eta,t} \sim i.i.d. \mathcal{N}(0, \mathbf{Id}_{n_\eta \times n_\eta}). \tag{S.1}$$

Renne: University of Lausanne, Quartier Chamberonne, CH-1015 Lausanne, Switzerland (email: jean-paul.renne@unil.ch); Chikhani: University of Lausanne (email: pauline.chikhani@unil.ch). This paper has circulated under two other titles: "Climate Linkers: Rationale and Pricing," and "Pricing Climate Linkers." We hereby declare that we have no known competing financial interests or personal relationships that could have appeared to influence the work reported in this paper. R codes for full reproduction of results are available here; a web interface is available here.

The components of the η_t vectors can serve multiple functions. They can be incorporated into certain model equations to account for additional sources of uncertainty; they might be included in the productivity specification A_t (equation 10) to introduce persistent (long-run risk) components. Alternatively, they could be used to enhance the specification of additional variables, such as inflation (see Subsection 4.3).

The dynamics of Z_t can still be concisely written in matrix form (as in Subsection C):

$$A_0^* Z_t = A_{1,t}^* Z_{t-1} + \omega_{0,t}^* + \omega_t^* W_t, \tag{S.2}$$

or

$$Z_t = A_{1,t} Z_{t-1} + \omega_{0,t} + \omega_t W_t, \tag{S.3}$$

with

$$A_{1,t} = (A_0^*)^{-1} A_{1,t}^*, \quad \omega_{0,t} = (A_0^*)^{-1} \omega_{0,t}^*, \quad \omega_t = (A_0^*)^{-1} \omega_t^*,$$

but the Laplace transforms of W_t is now different from the one given in Proposition 1.

The following proposition extends Proposition 1 to the case where η_t follows eq. S.1. (Consequently, the proof of Proposition 1 follows from the proof of Proposition 1, setting Φ to zero.)

Proposition 1. State vector dynamics.

The model described by equations (1) to (20), augmented with (S.1), is such that if $X_t = [Z_t' \, W_t']'$, *with* $Z_t = [\tilde{y}_t \, \mathcal{E}_t \, \mathcal{E}_{Ind,t} \, F_t \, M_{AT,t} \, M_{UP,t} \, M_{LO,t} \, T_{LO,t} \, H_t]'$ *and* $W_t = [\eta_{A,t} \, D_t \, N_t \, T_{AT,t} \, \Delta H_t]'$, *the conditional log Laplace transform of* X_t *is given by:*

$$\psi_t(u) := \log \mathbb{E}_t(\exp(u' X_{t+1})) = \alpha_t(u) + \beta_t(u)' X_t, \tag{S.4}$$

with

$$\begin{cases} \alpha_t(u) &= u_Z' \omega_{0,t+1} + \alpha_{W,t}(u_W + \omega_{t+1}' u_Z) \\ \beta_t(u) &= \begin{bmatrix} A_{1,t+1}' u_Z \\ 0_{n_W \times 1} \end{bmatrix} + \beta_{W,t}(u_W + \omega_{t+1}' u_Z), \end{cases} \tag{S.5}$$

where $u = [u_Z', u_W']'$ *and* n_W *is the dimension of* W_t. *Matrices* $A_{1,t}$, $\omega_{0,t}$, *and* ω_t *deterministically depend on time; they are such that* $Z_t = A_{1,t} Z_{t-1} + \omega_{0,t} + \omega_t W_t$, *and are detailed in Appendix C. Functions* $\alpha_{W,t}$ *and* $\beta_{W,t}$ *characterize the log Laplace transform of* W_t. *Specifically, for all* t, *we have:*

$$\psi_{W,t}(u_W) := \log \mathbb{E}_t(\exp[u_W' W_{t+1}]) = \alpha_W(u_W) + \beta_W(u_W)' X_t,$$

with $u_W = [u_\eta, u_D, u_N, u_T, u_H]'$ *and*

$$\begin{cases} \alpha_{W,t}(u_W) &= \frac{u_\eta^2}{2} + \frac{u_D\mu_D}{1-u_D\mu_D}\ell_0^{(D)} + \frac{u_N\mu_N}{1-u_N\mu_N}\ell_{0,t+1}^{(N)} + \frac{u_T\mu_T}{1-u_T\mu_T}\ell_0^{(T_{AT})} + \frac{u_H\mu_H}{1-u_H\mu_H}\ell_0^{(\Delta H)} \\ \beta_{W,t}(u_W) &= \begin{bmatrix} 0_{n_Z\times 1} \\ \Phi' u_\eta \\ 0_{(n_W-n_\eta)\times 1} \end{bmatrix} + \frac{u_D\mu_D}{1-u_D\mu_D}\ell_1^{(D)} + \frac{u_N\mu_N}{1-u_N\mu_N}\ell_{1,t+1}^{(N)} + \frac{u_T\mu_T}{1-u_T\mu_T}\ell_1^{(T_{AT})} + \frac{u_H\mu_H}{1-u_H\mu_H}\ell_1^{(\Delta H)}, \end{cases}$$

where scalars $\ell_{0,t}^{(w)}$ *and vectors* $\ell_{1,t}^{(w)}$ $(w \in \{D, N, T_{AT}, \Delta H\})$ *are such that* $w_t|\mathcal{I}_{t-1} \sim \gamma_0(\ell_{0,t}^{(w)} + \ell_{1,t}^{(w)'} X_{t-1}, \mu_w)$ *(see Table 6 in Appendix C for detailed specifications of the* ℓ_0*s and* ℓ_1*s.).*

Proof. The shocks being conditionally independent, and using the Laplace transform of the γ_0 distribution (Appendix A) used to model D_t and N_t (see eqs. 13 and 7), we have:

$$\begin{aligned} &\mathbb{E}_t\left(\exp\left(u_W' W_{t+1}\right)\right) = \mathbb{E}_t\left[\exp\left(u_\eta'\eta_{t+1} + u_D D_{t+1} + u_N N_{t+1}\right)\right] \\ =\ &\exp\left(u_\eta'\Phi\eta_t\right)\mathbb{E}_t\left(\exp\left(u_\eta'\varepsilon_{\eta,t+1}\right)\right) \times \\ &\mathbb{E}_t\left(\exp\left(u_D D_{t+1}\right)\right)\mathbb{E}_t\left(\exp\left(u_N N_{t+1}\right)\right)\mathbb{E}_t\left(\exp\left(u_T T_{AT,t+1}\right)\right)\mathbb{E}_t\left(\exp\left(u_H H_{t+1}\right)\right) \\ =\ &\exp\left[u_\eta'\Phi\eta_t + \frac{u_\eta u_\eta'}{2} + \frac{u_D\mu_D}{1-u_D\mu_D}\left(\ell_0^{(D)} + \ell_1^{(D)\prime} X_t\right) + \frac{u_N\mu_N}{1-u_N\mu_N}\left(\ell_{0,t+1}^{(N)} + \ell_{1,t+1}^{(N)\prime} X_t\right) + \right. \\ &\left. \frac{u_T\mu_T}{1-u_T\mu_T}\left(\ell_0^{(T_{AT})} + \ell_1^{(T_{AT})\prime} X_t\right) + \frac{u_H\mu_H}{1-u_H\mu_H}\left(\ell_0^{(\Delta H)} + \ell_1^{(\Delta H)\prime} X_t\right)\right], \end{aligned}$$

which gives the Laplace transform of W_t. Moreover, we have:

$$\begin{aligned} &\mathbb{E}_t(\exp(u' X_{t+1})) = \mathbb{E}_t[\exp(u_Z' Z_{t+1} + u_W' W_{t+1})] \\ =\ &\mathbb{E}_t(\exp(u_Z'(A_{1,t+1} Z_t + \omega_{0,t+1} + \omega_{t+1} W_{t+1}) + u_W W_{t+1})) \\ =\ &\exp\left[u_Z'(A_{1,t+1} Z_t + \omega_{0,t+1}) + \alpha_{W,t}\left(u_W + \omega_{t+1}' u_Z\right) + \beta_{W,t}\left(u_W + \omega_{t+1}' u_Z\right)' X_t\right], \end{aligned}$$

which leads to the result. □

S.A.2. **Proof of Proposition 2 (multi-horizon Laplace transform of X_t).**

Proof. We have:

$$\begin{aligned} &\mathbb{E}_t(\exp[u_1' X_{t+1} + \cdots + u_h' X_{t+h}]) \\ =\ &\mathbb{E}_t\left(\mathbb{E}_{t+1}(\exp[u_1' X_{t+1} + \cdots + u_h' X_{t+h}])\right) \\ =\ &\mathbb{E}_t\left(\exp\left[u_1' X_{t+1} + \psi_{0,t+1}^{(h-1)}(u_2, \ldots, u_h) + \psi_{1,t+1}^{(h-1)}(u_2, \ldots, u_h)' X_{t+1}\right]\right) \\ =\ &\exp\left[\psi_{0,t+1}^{(h-1)}(u_2, \ldots, u_h) + \alpha_t\left(u_1 + \psi_{1,t+1}^{(h-1)}(u_2, \ldots, u_h)\right) + \beta_t\left(u_1 + \psi_{1,t+1}^{(h-1)}(u_2, \ldots, u_h)\right)' X_t\right], \end{aligned}$$

which leads to the result by induction. □

In practice: Using the notation $U_k = \psi^{(k)}_{1,t+h-k}(u_{h-k+1}, \ldots, u_h)$ [in particular, $U_h = \psi^{(h)}_{1,t}(u_1, \ldots, u_h)$], the second equation of (26) implies that, for $k \geq 2$:

$$U_k = \beta_{t+h-k}(u_{h-k+1} + U_{k-1}),$$

which allows to compute the U_k ($k = 1, \ldots, h$) by backward recursions, starting from $U_1 = \beta_{t+h-1}(u_h)$. Once the U_k ($k = 1, \ldots, h$) are computed, the first equation of (26) gives $\psi^{(h)}_{0,t}(u_1, \ldots, u_h)$. Specifically, for $h \geq 1$, we have:

$$\psi^{(h)}_{0,t}(u_1, \ldots, u_h) = \alpha_t(u_1 + U_{h-1}) + \alpha_{t+1}(u_2 + U_{h-2}) + \cdots + \alpha_{t+h-2}(u_{h-1} + U_1) + \alpha_{t+h-1}(u_h).$$

Corollary 1. (Simple) multi-horizon Laplace transform of $X_t = [Z_t' \, W_t']'$. *Using the $\psi^{(h)}_t$ notation introduced in Proposition 2 (via eq. 25), we have:*

$$\psi^{(h)}_t(0, \ldots, 0, u) = \log \mathbb{E}_t(\exp(u' X_{t+h})) = a_{t,h}(u) + b_{t,h}(u)' X_t,$$

where $b_{t,k}(u) = \beta_t \circ \cdots \circ \beta_{t+k-1}(u)$, and

$$a_{t,h} = \alpha_{t+h-1}(u) + \alpha_{t+h-2}(b_{t+h-1,1}(u)) + \cdots + \alpha_{t+1}(b_{t+2,h-2}(u)) + \alpha_t(b_{t+1,h-1}(u)),$$

where functions α_s and β_s are defined in (22).

In practice: Using the notation $U_k = \psi^{(k)}_{1,t+h-k}(0, \ldots, 0, u)$ [in particular, $U_h = \psi^{(h)}_{1,t}(0, \ldots, 0, u) = b_{t,h}(u)$], the second equation of (26) implies that, for $k \geq 2$:

$$U_k = \beta_{t+h-k}(U_{k-1}),$$

which allows to compute the U_k ($k = 1, \ldots, h$) by backward recursions, starting from $U_1 = \beta_{t+h-1}(u)$. Once the U_k ($k = 1, \ldots, h$) are computed, the first equation of (26) gives $a_{t,h}(u) = \psi^{(h)}_{0,t}(u_1, \ldots, u_h)$. Specifically, for $h \geq 1$, we have:

$$a_{t,h}(u) = \alpha_t(U_{h-1}) + \alpha_{t+1}(U_{h-2}) + \cdots + \alpha_{t+h-2}(U_1) + \alpha_{t+h-1}(u).$$

S.A.3. **Conditional means and variances of $X_t = [Z_t' \, W_t']'$.** We start by establishing the conditional means and variances of W_t.

Proposition 2. *The conditional mean of W_{t+1}, given the information available at t, is given by:*

$$\mathbb{E}_t(W_{t+1}) = \alpha^{(1)}_{W,t} + \beta^{(1)}_{W,t} X_t, \tag{S.6}$$

where

$$\begin{cases} \alpha^{(1)}_{W,t} &= \left[\mathbf{0}'_{(n_Z+n_\eta)\times 1}\ \mu_D\ell_0^{(D)}\ \mu_N\ell_{0,t+1}^{(N)}\ \mu_D\ell_0^{(T_{AT})}\ \mu_D\ell_0^{(\Delta H)}\right]', \\ \beta^{(1)}_{W,t} &= \begin{bmatrix} \mathbf{0}_{n_Z\times n_Z} & \mathbf{0}_{n_Z\times n_\eta} & \mathbf{0}_{n_Z\times(n_W-n_\eta)} \\ \mathbf{0}_{n_\eta\times n_Z} & \Phi_{n_\eta\times n_\eta} & \mathbf{0}_{n_\eta\times(n_W-n_\eta)} \\ \mathbf{0}_{(n_W-n_\eta)\times n_Z} & \mathbf{0}_{(n_W-n_\eta)\times n_\eta} & \mathbf{0}_{(n_W-n_\eta)\times(n_W-n_\eta)} \end{bmatrix} + \mu_D \begin{bmatrix} \mathbf{0}_{(n_Z+n_\eta)\times n_X} \\ \ell_1^{(D)\prime} \\ \mathbf{0}_{3\times n_X} \end{bmatrix} \\ &\quad + \mu_N \begin{bmatrix} \mathbf{0}_{(n_Z+n_\eta)\times n_X} \\ \mathbf{0}_{1\times n_X} \\ \ell_{1,t+1}^{(N)\prime} \\ \mathbf{0}_{2\times n_X} \end{bmatrix} + \mu_T \begin{bmatrix} \mathbf{0}_{(n_Z+n_\eta)\times n_X} \\ \mathbf{0}_{2\times n_X} \\ \ell_1^{(T_{AT})\prime} \\ \mathbf{0}_{1\times n_X} \end{bmatrix} + \mu_H \begin{bmatrix} \mathbf{0}_{(n_Z+n_\eta)\times n_X} \\ \mathbf{0}_{3\times n_X} \\ \ell_1^{(\Delta H)\prime} \end{bmatrix}. \end{cases}$$

Proof. This directly results from the conditional expectations of the different entries of $W_t = [\eta_t', D_t, N_t, T_{AT,t+1}, \Delta H_{t+1}]'$. □

Proposition 3. *The conditional variance of W_{t+1}, given the information available at t, is given by:*

$$Vec\left(\mathbb{V}\mathrm{ar}_t(W_{t+1})\right) = \alpha^{(2)}_{W,t} + \beta^{(2)}_{W,t} X_t, \tag{S.7}$$

where $\beta^{(2)}_{W,t}$ is equal to

$$Vec\left(\begin{bmatrix} \mathbf{0}_{n_\eta\times n_\eta} & \mathbf{0}_{n_\eta\times 1} & \mathbf{0}_{n_\eta\times 1} & \mathbf{0}_{n_\eta\times 1} & \mathbf{0}_{n_\eta\times 1} \\ \mathbf{0}_{1\times n_\eta} & 2\mu_D^2 & 0 & 0 & 0 \\ \mathbf{0}_{1\times n_\eta} & 0 & 0 & 0 & 0 \\ \mathbf{0}_{1\times n_\eta} & 0 & 0 & 0 & 0 \\ \mathbf{0}_{1\times n_\eta} & 0 & 0 & 0 & 0 \end{bmatrix}\right) \ell_1^{(D)\prime} + Vec\left(\begin{bmatrix} \mathbf{0}_{n_\eta\times n_\eta} & \mathbf{0}_{n_\eta\times 1} & \mathbf{0}_{n_\eta\times 1} & \mathbf{0}_{n_\eta\times 1} & \mathbf{0}_{n_\eta\times 1} \\ \mathbf{0}_{1\times n_\eta} & 0 & 0 & 0 & 0 \\ \mathbf{0}_{1\times n_\eta} & 0 & 2\mu_N^2 & 0 & 0 \\ \mathbf{0}_{1\times n_\eta} & 0 & 0 & 0 & 0 \\ \mathbf{0}_{1\times n_\eta} & 0 & 0 & 0 & 0 \end{bmatrix}\right) \ell_{1,t+1}^{(N)\prime} +$$
$$Vec\left(\begin{bmatrix} \mathbf{0}_{n_\eta\times n_\eta} & \mathbf{0}_{n_\eta\times 1} & \mathbf{0}_{n_\eta\times 1} & \mathbf{0}_{n_\eta\times 1} & \mathbf{0}_{n_\eta\times 1} \\ \mathbf{0}_{1\times n_\eta} & 0 & 0 & 0 & 0 \\ \mathbf{0}_{1\times n_\eta} & 0 & 0 & 0 & 0 \\ \mathbf{0}_{1\times n_\eta} & 0 & 0 & 2\mu_T^2 & 0 \\ \mathbf{0}_{1\times n_\eta} & 0 & 0 & 0 & 0 \end{bmatrix}\right) \ell_1^{(T_{AT})\prime} + Vec\left(\begin{bmatrix} \mathbf{0}_{n_\eta\times n_\eta} & \mathbf{0}_{n_\eta\times 1} & \mathbf{0}_{n_\eta\times 1} & \mathbf{0}_{n_\eta\times 1} & \mathbf{0}_{n_\eta\times 1} \\ \mathbf{0}_{1\times n_\eta} & 0 & 0 & 0 & 0 \\ \mathbf{0}_{1\times n_\eta} & 0 & 0 & 0 & 0 \\ \mathbf{0}_{1\times n_\eta} & 0 & 0 & 0 & 0 \\ \mathbf{0}_{1\times n_\eta} & 0 & 0 & 0 & 2\mu_H^2 \end{bmatrix}\right) \ell_1^{(\Delta H)\prime},$$

and where

$$\alpha^{(2)}_{W,t} = Vec\left(\begin{bmatrix} \boldsymbol{Id}_{n_\eta\times n_\eta} & \mathbf{0}_{n_\eta\times 1} & \mathbf{0}_{n_\eta\times 1} & \mathbf{0}_{n_\eta\times 1} & \mathbf{0}_{n_\eta\times 1} & \mathbf{0}_{n_\eta\times 1} \\ \mathbf{0}_{1\times n_\eta} & 2\mu_D^2\ell_0^{(D)} & 0 & 0 & 0 & 0 \\ \mathbf{0}_{1\times n_\eta} & 0 & 2\mu_N^2\ell_{0,t+1}^{(N)} & 0 & 0 & 0 \\ \mathbf{0}_{1\times n_\eta} & 0 & 0 & 0 & 2\mu_T^2\ell_0^{(T_{AT})} & 0 \\ \mathbf{0}_{1\times n_\eta} & 0 & 0 & 0 & 0 & 2\mu_H^2\ell_0^{(\Delta H)} \end{bmatrix}\right).$$

Proof. The shocks being conditionally independent, it comes that $\mathbb{V}\mathrm{ar}_t\left(W_{t+1}\right)$ is a diagonal matrix whose diagonal entries are $\mathbb{V}\mathrm{ar}_t(\eta_{t+1})$, $\mathbb{V}\mathrm{ar}_t(D_{t+1})$, $\mathbb{V}\mathrm{ar}_t(N_{t+1})$, $\mathbb{V}\mathrm{ar}_t(T_{AT,t+1})$, and

$\mathbb{V}\text{ar}_t(H_{t+1})$. Using $\mathbb{V}\text{ar}_t(\eta_{t+1}) = \mathbf{Id}_{n_\eta \times n_\eta}$, as well as $\mathbb{V}\text{ar}_t(D_{t+1}) = 2\mu_D^2\left(\ell_0^{(D)} + \ell_1^{(D)\prime} X_t\right)$, $\mathbb{V}\text{ar}_t(N_{t+1}) = 2\mu_N^2\left(\ell_{0,t+1}^{(N)} + \ell_{1,t+1}^{(N)\prime} X_t\right)$, $\mathbb{V}\text{ar}_t(T_{AT,t+1}) = 2\mu_T^2\left(\ell_0^{(T_{AT})} + \ell_1^{(T_{AT})\prime} X_t\right)$, and $\mathbb{V}\text{ar}_t(H_{t+1}) = 2\mu_H^2\left(\ell_0^{(\Delta H)} + \ell_1^{(\Delta H)\prime} X_t\right)$ leads to the result. □

Proposition 4. *The conditional mean of X_{t+h}, given the information available at t, is given by:*

$$\mathbb{E}_t(X_{t+h}) = \alpha_{t,h}^{(1)} + \beta_{t,h}^{(1)} X_t, \tag{S.8}$$

where

$$\begin{cases} \alpha_{t,h}^{(1)} &= \mu_{X,t+h-1} + \Phi_{X,t+h-1}\mu_{X,t+h-2} + \cdots + \Phi_{X,t+1}^{h-1}\mu_{X,t}, \\ \beta_{t,h}^{(1)} &= \Phi_{X,t+h-1}\Phi_{X,t+h-2}\cdots\Phi_{X,t}, \end{cases}$$

with

$$\mu_{X,t} = \begin{bmatrix} \omega_{0,t+1} \\ \mathbf{0}_{n_W \times 1} \end{bmatrix} + \begin{bmatrix} \mathbf{0}_{n_Z \times n_Z} & \omega_{t+1} \\ \mathbf{0}_{n_W \times n_Z} & \boldsymbol{Id}_{n_W \times n_W} \end{bmatrix} \alpha_{W,t}^{(1)}, \quad \textit{and}$$

$$\Phi_{X,t} = \begin{bmatrix} A_{1,t+1} & \mathbf{0}_{n_Z \times n_W} \\ \mathbf{0}_{n_W \times n_Z} & \mathbf{0}_{n_W \times n_W} \end{bmatrix} + \begin{bmatrix} \mathbf{0}_{n_Z \times n_Z} & \omega_{t+1} \\ \mathbf{0}_{n_W \times n_Z} & \boldsymbol{Id}_{n_W \times n_W} \end{bmatrix} \beta_{W,t}^{(1)}.$$

Proof. Using (S.3), we have:

$$X_{t+1} = \begin{bmatrix} Z_{t+1} \\ W_{t+1} \end{bmatrix} = \begin{bmatrix} A_{1,t+1}Z_t + \omega_{0,t+1} + \omega_{t+1}W_{t+1} \\ W_{t+1} \end{bmatrix}, \tag{S.9}$$

and therefore $\mathbb{E}_t(X_{t+1}) = \begin{bmatrix} A_{1,t+1}Z_t + \omega_{0,t+1} \\ \mathbf{0}_{n_W \times 1} \end{bmatrix} + \begin{bmatrix} \mathbf{0}_{n_Z \times n_Z} & \omega_{t+1} \\ \mathbf{0}_{n_W \times n_Z} & \mathbf{Id}_{n_W \times n_W} \end{bmatrix} (\alpha_{W,t}^{(1)} + \beta_{W,t}^{(1)} X_t)$, which gives the result for $h = 1$.

The law of iterated expectation implies that the conditional expectation $\mathbb{E}_t(X_{t+h})$ is given by $\mathbb{E}_t(X_{t+h}) = \mu_{X,t+h-1} + \Phi_{X,t+h-1}\mathbb{E}_t(X_{t+h-1})$, which leads to the result. □

Proposition 5. *The conditional variance of X_{t+h}, given the information available at t, is given by:*

$$Vec\left(\mathbb{V}ar_t(X_{t+h})\right) = \alpha_{t,h}^{(2)} + \beta_{t,h}^{(2)} X_t, \tag{S.10}$$

where

$$\begin{cases} \alpha_{t,h}^{(2)} = \alpha_{t+h-1,1}^{(2)} + \beta_{t+h-1,1}^{(2)}\alpha_{t,h-1}^{(1)} + \left(\beta_{t+h-1,1}^{(1)} \otimes \beta_{t+h-1,1}^{(1)}\right)\alpha_{t,h-1}^{(2)} \\ \beta_{t,h}^{(2)} = \beta_{t+h-1,1}^{(2)}\beta_{t,h-1}^{(1)} + \left(\beta_{t+h-1,1}^{(1)} \otimes \beta_{t+h-1,1}^{(1)}\right)\beta_{t,h-1}^{(2)}, \end{cases} \tag{S.11}$$

with

$$\begin{cases} \alpha_{s,1}^{(2)} = \left(\Gamma_s \otimes \Gamma_s\right)\alpha_{W,t}^{(2)} \\ \beta_{s,1}^{(2)} = \left(\Gamma_s \otimes \Gamma_s\right)\beta_{W,t}^{(2)} \end{cases}, \quad \textit{where } \Gamma_s = \begin{bmatrix} \omega_{s+1} \\ \boldsymbol{Id}_{n_W \times n_W} \end{bmatrix}. \tag{S.12}$$

Proof. Let us start with the case $h = 1$. Using (S.9), we have:

$$\mathbb{V}\text{ar}_t(X_{t+1}) = \mathbb{V}\text{ar}_t\left(\begin{bmatrix} \omega_{t+1} \\ \mathbf{Id}_{n_W \times n_W} \end{bmatrix} W_{t+1}\right) = \Gamma_t \mathbb{V}\text{ar}_t(W_{t+1})\Gamma_{t+1}',$$

where $\mathbb{V}\text{ar}_t(W_{t+1})$ is given by (S.7). This implies that:

$$Vec\left(\mathbb{V}\text{ar}_t(X_{t+1})\right) = (\Gamma_{t+1} \otimes \Gamma_{t+1}) Vec\left(\mathbb{V}\text{ar}_t(W_{t+1})\right) = (\Gamma_{t+1} \otimes \Gamma_{t+1})\left(\alpha^{(2)}_{W,t} + \beta^{(2)}_{W,t} X_t\right),$$

where the last equality is obtained by applying Proposition 3. This proves (S.10) for $h = 1$ (using S.12). Let us make the inductive hypothesis that (S.10) holds for $h-1$. More precisely, assume that, for any date t: $\text{Vec}\left(\mathbb{V}ar_t(X_{t+h-1})\right) = \alpha^{(2)}_{t,h-1} + \beta^{(2)}_{t,h-1} X_t$. The law of total variance yields:

$$\mathbb{V}ar_t(X_{t+h}) = \mathbb{E}_t(\mathbb{V}ar_{t+h-1}(X_{t+h})) + \mathbb{V}ar_t(\mathbb{E}_{t+h-1}(X_{t+h})).$$

We get:

$$\begin{aligned}
&\text{Vec}\left(\mathbb{V}ar_t(X_{t+h})\right) \\
=\ & \mathbb{E}_t\Big(\underbrace{\alpha^{(2)}_{t+h-1,1} + \beta^{(2)}_{t+h-1,1} X_{t+h-1}}_{\text{using the inductive hypothesis}} \Big) + \text{Vec}\Big(\mathbb{V}ar_t\Big(\underbrace{\alpha^{(1)}_{t+h-1,1} + \beta^{(1)}_{t+h-1,1} X_{t+h-1}}_{\text{using (S.8)}} \Big)\Big) \\
=\ & \alpha^{(2)}_{t+h-1,1} + \beta^{(2)}_{t+h-1,1}\Big(\underbrace{\alpha^{(1)}_{t,h-1} + \beta^{(1)}_{t,h-1} X_t}_{\text{using (S.8)}} \Big) + \text{Vec}\Big(\beta^{(1)}_{t+h-1,1} \mathbb{V}ar_t(X_{t+h-1}) {\beta^{(1)}_{t+h-1,1}}'\Big) \\
=\ & \alpha^{(2)}_{t+h-1,1} + \beta^{(2)}_{t+h-1,1}\alpha^{(1)}_{t,h-1} + \beta^{(2)}_{t+h-1,1}\beta^{(1)}_{t,h-1} X_t + \left(\beta^{(1)}_{t+h-1,1} \otimes \beta^{(1)}_{t+h-1,1}\right) \text{Vec}\left(\mathbb{V}ar_t(X_{t+1})\right) \\
=\ & \alpha^{(2)}_{t+h-1,1} + \beta^{(2)}_{t+h-1,1}\alpha^{(1)}_{t,h-1} + \beta^{(2)}_{t+h-1,1}\beta^{(1)}_{t,h-1} X_t + \left(\beta^{(1)}_{t+h-1,1} \otimes \beta^{(1)}_{t+h-1,1}\right)\left(\alpha^{(2)}_{t,h-1} + \beta^{(2)}_{t,h-1} X_t\right),
\end{aligned}$$

using (S.10) for $h = 1$.

To summarize, we have shown that: (S.10) is satisfied for $h = 1$, and that, if it is satisfied for $h-1$ (with $h \geq 2$), then it is also satisfied for h (see eq. S.10). By induction, it comes that it is satisfied for any $h \geq 1$. □

In practice, in order to use (S.11), we need: $\alpha^{(2)}_{t+k,1}$, $\beta^{(2)}_{t+k,1}$ for all k of interest, using (S.12); $\alpha^{(1)}_{t+k,1} \equiv \mu_{X,t+k}$, $\beta^{(1)}_{t+k,1} \equiv \Phi_{X,t+k}$ for all k of interest; $\alpha^{(1)}_{t,k}$, $\beta^{(1)}_{t,k}$ for all k of interest, using (S.8).

S.B. Pricing

S.B.1. **Proof of Proposition 3 (utility function).**

Proof. We start by positing a specification for the log-utility of the form of (29). Our objective is to determine whether a utility of this form can satisfy (15), and the conditions that then have

to be satisfied by $\mu_{u,0,t}$ and $\mu_{u,1,t}$. Under (29), we have:

$$\begin{aligned}
& \mathbb{E}_t \exp\left[(1-\gamma)u_{t+1}\right] \\
= \; & \mathbb{E}_t \exp\left[(1-\gamma)(c_{t+1}+\mu_{u,0,t+1}+\mu'_{u,1,t+1}X_{t+1})\right] \\
= \; & \mathbb{E}_t \exp\left[(1-\gamma)(c_t+\Delta c_{t+1}+\mu_{u,0,t+1}+\mu'_{u,1,t+1}X_{t+1})\right] \\
= \; & \exp\left[(1-\gamma)(c_t+\mu_{u,0,t+1}+\mu_{c,0,t+1})\right] \times \mathbb{E}_t \exp\left[(1-\gamma)(\mu_{u,1,t+1}+\mu_{c,1,t+1})'X_{t+1}\right] \\
= \; & \exp\left[(1-\gamma)(c_t+\mu_{u,0,t+1}+\mu_{c,0,t+1})\right] \times \\
& \exp\left[\alpha_t\{(1-\gamma)(\mu_{u,1,t+1}+\mu_{c,1,t+1})+\beta_t\{(1-\gamma)(\mu_{u,1,t+1}+\mu_{c,1,t+1})\}'X_t\right].
\end{aligned}$$

Substituting for $\mathbb{E}_t \exp\left[(1-\gamma)u_{t+1}\right]$ in (15) gives:

$$\begin{aligned}
u_t \; = \; & c_t+\delta(\mu_{u,0,t+1}+\mu_{c,0,t+1})+ \\
& \frac{\delta}{1-\gamma}\Big(\alpha_t\{(1-\gamma)(\mu_{u,1,t+1}+\mu_{c,1,t+1})\}+\beta_t\{(1-\gamma)(\mu_{u,1,t+1}+\mu_{c,1,t+1})\}'X_t\Big).
\end{aligned}$$

Therefore, for u_t to be equal to $c_t+\mu_{u,0,t}+\mu'_{u,1,t}X_t$, (32) has to be satisfied.

Eqs. (30) and (31) are obtained by setting $\mu_{u,1}=\mu_{u,1,t}=\mu_{u,1,t+1}$ and $\mu_{u,0}=\mu_{u,0,t}=\mu_{u,0,t+1}$ in (32). □

S.B.2. **Proof of Proposition 4 (SDF solution).**

Proof. When agents' preferences are as in (15), the SDF is given by (e.g. Piazzesi and Schneider, 2007):

$$\mathcal{M}_{t,t+1}=\delta\left(\frac{C_{t+1}}{C_t}\right)^{-1}\frac{\exp[(1-\gamma)u_{t+1}]}{\mathbb{E}_t(\exp[(1-\gamma)u_{t+1}])}.$$

Therefore, we have:

$$\begin{aligned}
\log\mathcal{M}_{t,t+1} \; = \; & \log\delta-\Delta c_{t+1}+(1-\gamma)u_{t+1}-\log\mathbb{E}_t(\exp[(1-\gamma)u_{t+1}]) \\
= \; & \log\delta-\Delta c_{t+1}+(1-\gamma)(c_t+\Delta c_{t+1}+\mu_{u,0,t+1}+\mu'_{u,1,t+1}X_{t+1}) \\
& -(1-\gamma)(c_t+\mu_{u,0,t+1}+\mu_{c,0,t+1}) \\
& -\alpha_t\{(1-\gamma)(\mu_{u,1,t+1}+\mu_{c,1,t+1})\}-\beta_t\{(1-\gamma)(\mu_{u,1,t+1}+\mu_{c,1,t+1})\}'X_t \\
= \; & \log\delta-\mu_{c,0,t+1}-\alpha_t\{(1-\gamma)(\mu_{u,1,t+1}+\mu_{c,1,t+1})\} \\
& +\Big((1-\gamma)\mu_{u,1,t+1}-\gamma\mu_{c,1,t+1}\Big)'X_{t+1}-\beta_t\{(1-\gamma)(\mu_{u,1,t+1}+\mu_{c,1,t+1})\}'X_t,
\end{aligned}$$

which leads to the result. □

S.B.3. **Proof of Proposition 5 (price of an asset whose payoff is $\exp(\omega'X_{t+h})$).**

Proof. The price of this asset is given by:

$$\mathbb{E}_t\left(\mathcal{M}_{t,t+h}\exp(\omega'X_{t+h})\right)$$

$$
\begin{aligned}
&= \mathbb{E}_t\Big\{\exp\Big(-\big[\mu_{r,0,t+1}+\alpha_t(\Pi_{t+1})+\{\mu_{r,1,t+1}+\beta_t(\Pi_{t+1})\}'X_t\big]\\
&\quad -\big[\mu_{r,0,t+2}+\alpha_{t+1}(\Pi_{t+2})+\{\mu_{r,1,t+2}+\beta_{t+1}(\Pi_{t+2})\}'X_{t+1}\big]+\Pi'_{t+1}X_{t+1}\\
&\quad \dots\\
&\quad -\big[\mu_{r,0,t+h}+\alpha_{t+h-1}(\Pi_{t+h})+\{\mu_{r,1,t+h}+\beta_{t+h-1}(\Pi_{t+h})\}'X_{t+h-1}\big]+\Pi'_{t+h-1}X_{t+h-1}\\
&\quad +\Pi'_{t+h}X_{t+h}+\omega'X_{t+h}\Big)\Big\}\\
&= \exp(-\mu_{r,0,t+1}-\alpha_t(\Pi_{t+1})-\cdots-\mu_{r,0,t+h}-\alpha_{t+h-1}(\Pi_{t+h}))\times\\
&\quad \exp(-\{\mu_{r,1,t+1}+\beta_t(\Pi_{t+1})\}'X_t)\exp\left[\psi^{(h)}_{0,t}(u_1,\dots,u_h)+\psi^{(h)}_{1,t}(u_1,\dots,u_h)'X_t\right],
\end{aligned}
$$

where functions $\psi^{(h)}_{0,t}$ and $\psi^{(h)}_{1,t}$ are defined in (26) and the u_k's are given in (36). □

S.C. CALIBRATION

S.C.1. **Outline of the calibration strategy.** This appendix describes the calibration of three sets of parameters, which respectively characterize: damages (Subsection S.C.2), the permafrost-related carbon release (Subsection S.C.3), and sea level rise (Subsection S.C.4). In these three cases, we adopt the same general approach. For a number k of parameters to calibrate, we consider k targeted moments and deduce the parameters to perfectly match these moments. The literature usually offers targets in the form of moments that are conditional on a given atmospheric temperature $T_{AT,t}$ on a given date (often 2100, that is $t = t_{2100}$, say). For instance, we may want our model to be such that global mean sea levels rise by X_1 meters if the atmospheric temperature is of T_1°C in 2100, and by X_2 meters if the temperature is of T_2°C. That is:

$$\mathbb{E}_0(H_{t_{2100}}|T_{AT,t_{2100}}=T_i)=X_i,\quad i\in\{1,2\}.$$

Even in a tractable model such as ours, the previous conditional expectation is complicated to calculate because the conditioning information set is not a temperature trajectory but a terminal condition on $T_{AT,t_{2100}}$. Such a conditional moment can however be computed if we condition on a trajectory of temperatures $\underline{T_{AT,t_{2100}}}$, with $\underline{T_{AT,t_{2100}}}=\{T_{AT,0},\dots,T_{AT,t_{2100}}\}$. Moreover, if we consider a parametric trajectory, we can obtain closed-form expressions for such moments, which facilitates the calibration. Observing that IAMs generally generate concave temperature trajectories, we employ the following parametric trajectory:

$$T_{AT,i}=\underbrace{T_\infty-(T_\infty-T_{AT,0})\exp(-\alpha i)}_{=:\mathcal{T}_i(T_\infty)},\quad i\in\{0,\dots,t_{2100}\},\tag{S.13}$$

where $\alpha>0$ is a convexity term. The numerical α value is obtained so as to minimized the squared deviation between the parametric trajectory (S.13) and the average of the RCP4.5 and RCP6.0 temperature trajectories; this gives $\alpha=0.03$.

We emphasize that this parametric trajectory is used solely for calibration purposes; our model does not restrict temperature to adhere to this parametric trajectory.

We denote by $T_\infty(T_{AT,t_{2100}})$ the value of T_∞ that is such that $\mathcal{T}_{t_{2100}}(T_\infty(T_{AT,t_{2100}})) = T_{AT,t_{2100}}$. That is, if $T_\infty = T_\infty(T_{AT,t_{2100}})$, then the parametric temperature trajectory defined by (S.13) is such that atmospheric temperature is $T_{AT,t_{2100}}$ on date t_{2100}. Manipulating (S.13), we obtain:[1]

$$T_\infty(x) = \frac{x - T_{AT,0}e^{-\alpha t_{2100}}}{1 - e^{-\alpha t_{2100}}}.$$

Using the definition of $\mathcal{T}_i(T_\infty)$ (see eq. S.13), we have:

$$\mathcal{T}_0(T_\infty) + \cdots + \mathcal{T}_{t_{2100}-1}(T_\infty) = t_{2100}T_\infty - (T_\infty - T_{AT,0})\frac{1 - e^{-\alpha t_{2100}}}{1 - \exp(-\alpha)}.$$

If we want to compute this sum for a trajectory of temperatures that is such that $T_{AT,t_{2100}} = x$, we need to replace T_∞ with $T_\infty(x)$, which gives:

$$\begin{aligned} & \mathcal{T}_0(T_\infty(x)) + \cdots + \mathcal{T}_{t_{2100}-1}(T_\infty(x)) \qquad \text{(S.14)} \\ = \; & t_{2100}\frac{x - T_{AT,0}e^{-\alpha t_{2100}}}{1 - e^{-\alpha t_{2100}}} - \frac{x - T_{AT,0}}{1 - \exp(-\alpha)} \\ = \; & \underbrace{x\,\frac{t_{2100}(1 - \exp(-\alpha)) - (1 - e^{-\alpha t_{2100}})}{(1 - e^{-\alpha t_{2100}})(1 - \exp(-\alpha))}}_{:=a^*_\alpha} + T_{AT,0}\,\underbrace{\frac{1 - e^{-\alpha t_{2100}} - t_{2100}e^{-\alpha t_{2100}}(1 - \exp(-\alpha))}{(1 - e^{-\alpha t_{2100}})(1 - \exp(-\alpha))}}_{:=a^0_\alpha}. \end{aligned}$$

In the following, we explain how to obtain the distributions (and, therefore, moments) of cumulated damages, cumulated permafrost-related emissions, and sea level rises, conditional on such trajectories of atmospheric temperatures. Unlike simulation-based methods, these calibration approaches are immediate.

S.C.2. **Damages.** Under our assumptions, damages affect consumption growth (see eq. 18). This implies that the ratio between actual output (Y_t) and the output that would prevail in the absence of damages is $\exp(-\sum_{i=1}^t \mathcal{D}_i)$.[2]

According to (13), and assuming that the shocks are independent of one another, we have:

$$D_1 + \cdots + D_{t_{2100}} | \underline{T_{AT,t_{2100}}} \sim \gamma_0\left(\frac{1}{\mu_D}\left[t_{2100}a^{(D)} + b^{(D)}(T_{AT,0} + \cdots + T_{AT,t_{2100}-1})\right], \mu_D\right).$$

[1] It can be noted that we obtain a linear trajectory when $\alpha \to 0$; specifically, in that case, (S.13) becomes $\mathcal{T}_i(T_\infty(x)) = T_{AT,0} + \frac{i}{t_{2100}}(x - T_{AT,0})$.

[2] Denote total consumption growth damage by $\mathcal{D}_t$, i.e., $\mathcal{D}_t = D_t + b_{SK}\Delta H_t$. Denoting logarithm with small letters, our model implies that capital (log) growth is given by $\Delta k_t = \Delta c_{t-1} - \Delta\mathcal{D}_t$, where we have used that consumption C and planned capital K^* have the same growth rate in our model (with a one-period lag), see Footnote 16. Hence, since Δc_t is of the form $\mu_{c,t} - \mathcal{D}_t$ (where $\mu_{c,t}$ is exogenous), it comes that $\Delta k_t = \mu_{c,t-1} - \mathcal{D}_{t-1} - \Delta\mathcal{D}_t = \mu_{c,t-1} - \mathcal{D}_t$. As a result, the ratio between the actual capital and the capital that would prevail absent climate damages is equal to $\exp(-\sum_{i=1}^t \mathcal{D}_i)$. This is therefore also the case for output in our AK economy, where $Y_t = A_tK_t$ (A_t being exogenous).

Using the parametric trajectory (S.13), and imposing that $T_{AT,t_{2100}} = x$, we obtain:

$$D_1 + \cdots + D_{t_{2100}} | \underline{T_{AT,t_{2100}}} = \underline{\mathcal{T}_{t_{2100}}}(T_\infty(x)) \sim \gamma_0 \left(\frac{1}{\mu_D} \left\{ t_{2100} a^{(D)} + b^{(D)} [a_\alpha^* x + a_\alpha^0 T_{AT,0}] \right\}, \mu_D \right). \tag{S.15}$$

This determines the distribution of $\sum_{t=1}^{t_{2100}} D_t$, conditional on $\underline{T_{AT,t_{2100}}} = \underline{\mathcal{T}_{t_{2100}}}(T_\infty(x))$. Using (51), we obtain the following conditional Laplace transform for $\sum_{t=1}^{t_{2100}} D_t$:

$$\begin{aligned} &\mathbb{E}_0 \left(\exp\left(u \sum_{t=1}^{t_{2100}} D_t \right) \middle| \underline{T_{AT,t_{2100}}} = \underline{\mathcal{T}_{t_{2100}}}(T_\infty(x)) \right) \\ = \;& \exp\left(\frac{u}{1+u\mu_D} \left(a^{(D)} t_{2100} + b^{(D)} [a_\alpha^* x + a_\alpha^0 T_{AT,0}] \right) \right). \end{aligned} \tag{S.16}$$

Assume we target a specific mean ($\overline{\mathbb{E}}_{0,D}$) and variance ($\overline{\mathbb{V}\mathrm{ar}}_{0,D}$) of cumulated damages for a given trajectory of temperatures between dates 0 and t^*, i.e.,

$$\mathbb{E}_0 \left(\exp\left(- \sum_{t=1}^{t_{2100}} D_t \right) \middle| \underline{T_{AT,t_{2100}}} \right) = \overline{\mathbb{E}}_{0,D}, \quad \text{and} \quad \mathbb{V}ar_0 \left(\exp\left(- \sum_{t=1}^{t_{2100}} D_t \right) \middle| \underline{T_{AT,t_{2100}}} \right) = \overline{\mathbb{V}\mathrm{ar}}_{0,D}.$$

It can be shown that this is satisfied for:[3]

$$\mu_D = \left(1 - \frac{\log\left(\overline{\mathbb{V}\mathrm{ar}}_{0,D} + \left[\overline{\mathbb{E}}_{0,D} \right]^2 \right)}{2 \log\left(\overline{\mathbb{E}}_{0,D} \right)} \right) \Big/ \left(\frac{\log\left(\overline{\mathbb{V}\mathrm{ar}}_{0,D} + \left[\overline{\mathbb{E}}_{0,D} \right]^2 \right)}{\log\left(\overline{\mathbb{E}}_{0,D} \right)} - 1 \right).$$

Next, using (S.16) with $u = -1$), it appears that the (log) expected cumulated damages are linear in $\{a^{(D)}, b^{(D)}\}$ conditional on a given trajectory of temperatures. Hence, if we target two different conditional expectations ($\overline{\mathbb{E}}_{0,D,1}$ and $\overline{\mathbb{E}}_{0,D,2}$, say) for two different terminal values of $T_{AT,t_{2100}}$ ($T_{AT,t_{2100},1}$ and $T_{AT,t_{2100},2}$, say), we simply obtain $\{a^{(D)}, b^{(D)}\}$ by solving a two-equation linear system:

$$\begin{bmatrix} a^{(D)} \\ b^{(D)} \end{bmatrix} = -(1+\mu_D) \begin{bmatrix} t_{2100} & [a_\alpha^* T_{AT,t_{2100},1} + a_\alpha^0 T_{AT,0}] \\ t_{2100} & [a_\alpha^* T_{AT,t_{2100},2} + a_\alpha^0 T_{AT,0}] \end{bmatrix}^{-1} \begin{bmatrix} \log(\overline{\mathbb{E}}_{0,D,1}) \\ \log(\overline{\mathbb{E}}_{0,D,2}) \end{bmatrix}.$$

S.C.3. **Permafrost-related emissions.** According to (7), permafrost-related emissions are given by:

$$N_t | \underline{T_{AT,t}} \sim \gamma_0 \left(\frac{\kappa_N^{t-1}}{\mu_N} \left[a^{(N)} + b^{(N)} T_{AT,t-1} \right], \mu_N \right).$$

[3] Using that $\overline{\mathbb{E}}_{0,D} = \mathbb{E}_0 \left(\exp(-Cum_{D,t^*}) | \underline{T_{AT,t_{2100}}} \right)$ and that $\overline{\mathbb{V}\mathrm{ar}}_{0,D} = \mathbb{E}_0 \left(\exp(-2Cum_{D,t^*}) | \underline{T_{AT,t_{2100}}} \right) - \overline{\mathbb{E}}_{0,D}^2$, we obtain $\overline{\mathbb{V}\mathrm{ar}}_{0,D} + \left[\overline{\mathbb{E}}_{0,D} \right]^2 = \overline{\mathbb{E}}_{0,D}^{\frac{2(1+\mu_D)}{1+2\mu_D}}$, which gives the result.

The properties of the gamma distribution imply that:

$$N_t + \cdots + N_1 | \underline{T_{AT,t}} \sim \gamma_0 \left(\frac{1}{\mu_N} \left[\frac{1-\kappa_N^t}{1-\kappa_N} a^{(N)} + b^{(N)} \sum_{i=1}^{t} \kappa_N^{i-1} T_{AT,i-1} \right], \mu_N \right).$$

Using the parametric trajectory (S.13), and imposing that $T_{AT,t_{2100}} = x$, we obtain:

$$N_t + \cdots + N_1 | \underline{T_{AT,t}} = \underline{\mathcal{T}_t}(T_\infty(x)) \sim \gamma_0 \left(\frac{a^{(N)}}{\mu_N} \frac{1-\kappa_N^t}{1-\kappa_N} + \frac{b^{(N)}}{\mu_N} \sum_{i=1}^{t} \kappa_N^{i-1} \mathcal{T}_{i-1}(T_\infty), \mu_N \right).$$

We have:

$$\begin{aligned} \sum_{i=1}^{t} \kappa_N^{i-1} \mathcal{T}_{i-1}(T_\infty) &= \sum_{i=0}^{t-1} \kappa_N^i \left(T_\infty - (T_\infty - T_{AT,0}) \exp(-\alpha i) \right) \\ &= T_\infty \frac{1-\kappa_N^t}{1-\kappa_N} - (T_\infty - T_{AT,0}) \frac{1-\kappa_N^t e^{-\alpha t}}{1-\kappa_N e^{-\alpha}}. \end{aligned} \tag{S.17}$$

If, in the context of the parametric trajectory (S.13), we impose $T_{AT,t_{2100}} = x$, (S.17) becomes

$$\begin{aligned} \sum_{i=1}^{t} \kappa_N^{i-1} \mathcal{T}_{i-1}(T_\infty(x)) &= \frac{x - T_{AT,0} e^{-\alpha t_{2100}}}{1 - e^{-\alpha t_{2100}}} \times \frac{1-\kappa_N^t}{1-\kappa_N} - \frac{x - T_{AT,0}}{1 - e^{-\alpha t_{2100}}} \times \frac{1-\kappa_N^t e^{-\alpha t}}{1-\kappa_N e^{-\alpha}} \\ &= x b^*_{\alpha,t} + T_{AT,0} b^0_{\alpha,t}, \end{aligned}$$

where

$$\begin{cases} b^*_{\alpha,t} &= \frac{1}{1-e^{-\alpha t_{2100}}} \left(\frac{1-\kappa_N^t}{1-\kappa_N} - \frac{1-\kappa_N^t e^{-\alpha t}}{1-\kappa_N e^{-\alpha}} \right) \\ b^0_{\alpha,t} &= \frac{1}{1-e^{-\alpha t_{2100}}} \left(\frac{1-\kappa_N^t e^{-\alpha t}}{1-\kappa_N e^{-\alpha}} - \frac{(1-\kappa_N^t) e^{-\alpha t_{2100}}}{1-\kappa_N} \right). \end{cases}$$

As in Subsection S.C.2, targeting a specific variance-to-expectation ratio, conditionally on a given trajectory of temperatures between dates 1 and t_{2100}, gives μ_N. Indeed, using (52), we obtain:

$$\mu_N = \frac{\overline{\mathbb{V}ar}_0(N_1 + \cdots + N_{t_{2100}} | \underline{T_{AT,t_{2100}}})}{2\overline{\mathbb{E}}_0(N_1 + \cdots + N_{t_{2100}} | \underline{T_{AT,t_{2100}}})}. \tag{S.18}$$

Moreover, $\mathbb{E}_0(N_1 + \cdots + N_{t_{2100}} | \underline{T_{AT,t_{2100}}} = \underline{\mathcal{T}_{t_{2100}}}[T_\infty(x)])$ is a linear function of $\{a^{(N)}, b^{(N)}\}$:

$$\begin{aligned} &\mathbb{E}_0(N_1 + \cdots + N_{t_{2100}} | \underline{T_{AT,t_{2100}}} = \underline{\mathcal{T}_{t_{2100}}}[T_\infty(x)]) \\ &= \frac{1-\kappa_N^{t_{2100}}}{1-\kappa_N} a^{(N)} + (b^0_{\alpha,t_{2100}} T_{AT,0} + b^*_{\alpha,t_{2100}} x) b^{(N)}. \end{aligned} \tag{S.19}$$

Hence, for a given κ_N, one can solve for $\{a^{(N)}, b^{(N)}\}$ as soon as one targets a pair of conditional expectations (conditional on two different values of x).

A last moment we want to match is the expected total amount of carbon trapped in the permafrost. Assuming that the temperature will stabilize around T_∞, and under the parametric trajectory (S.13), this amount should be close to $\lim_{t\to\infty} \mathbb{E}_0(N_1 + \cdots + N_t | \underline{T_{AT,t}} = \underline{\mathcal{T}_t}[T_\infty])$.

Under (S.17), this (limit) expectation is given by:

$$\lim_{t\to\infty} \mathbb{E}_0(N_1 + \cdots + N_t | \underline{T_{AT,t}} = \underline{\mathcal{T}_t}[T_\infty]) = \frac{a^{(N)}}{1-\kappa_N} + \frac{b^{(N)} T_\infty}{1-\kappa_N} - \frac{b^{(N)}(T_\infty - T_{AT,0})}{1-\kappa_N e^{-\alpha}}. \tag{S.20}$$

To summarize, the set of parameters $\{\mu_N, \kappa_N, a^{(N)}, b^{(N)}\}$ is obtained as follows:

- Obtain μ_N through (S.18).
- Consider a grid of values for κ_N. For each value:
  - Compute $a^{(N)}$ and $b^{(N)}$ using (S.19), for two different values x of $T_{AT,t_{2100}}$.
  - Use (S.20) to compute $\lim_{t\to\infty} \mathbb{E}_0(N_1 + \cdots + N_t | \underline{T_{AT,t}} = \underline{\mathcal{T}_t}[T_\infty])$ for the desired T_∞ value.
- Select, within the grid, the value of κ_N that provides the best match of the targeted $\lim_{t\to\infty} \mathbb{E}_0(N_1 + \cdots + N_t | \underline{T_{AT,t}} = \underline{\mathcal{T}_t}[T_\infty])$, for the desired T_∞ value.

S.C.4. **Sea levels.** Using the dynamics of global mean sea level H_t described by (8) and conditional on the parametric trajectory (S.13) for $T_{AT,t}$, with $T_{AT,t_{2100}} = x$, (S.14) gives:

$$H_{t_{2100}} - H_0 | \underline{T_{AT,t_{2100}}} = \underline{\mathcal{T}_{t_{2100}}}(T_\infty(x)) \sim \gamma_0 \left(\frac{1}{\mu_H} \left\{ t_{2100} a^{(\Delta H)} + b^{(\Delta H)} [a_\alpha^* x + a_\alpha^0 T_{AT,0}] \right\}, \mu_H \right). \tag{S.21}$$

This implies in particular that

$$\mathbb{E}_0(H_{t_{2100}} | \underline{T_{AT,t_{2100}}} = \underline{\mathcal{T}_{t_{2100}}}(T_\infty(x))) \quad = \quad H_0 + t_{2100} a^{(\Delta H)} + b^{(\Delta H)} [a_\alpha^* x + a_\alpha^0 T_{AT,0}]. \tag{S.22}$$

Hence, $\mathbb{E}_0(H_{t_{2100}})$ is an affine function of $a^{(\Delta H)}$ and $b^{(\Delta H)}$. As a result, if we want to target two different sea levels ($\overline{H}_1$ and $\overline{H}_2$, say), for two different temperatures ($T_{AT,t_{2100},1}$ and $T_{AT,t_{2100},2}$, say), we obtain $\{a^{(\Delta H)}, b^{(\Delta H)}\}$ by solving a two-equation linear system, leading to:

$$\begin{bmatrix} a^{(\Delta H)} \\ b^{(\Delta H)} \end{bmatrix} = \begin{bmatrix} t_{2100} & [a_\alpha^* T_{AT,t_{2100},1} + a_\alpha^0 T_{AT,0}] \\ t_{2100} & [a_\alpha^* T_{AT,t_{2100},2} + a_\alpha^0 T_{AT,0}] \end{bmatrix}^{-1} \begin{bmatrix} \overline{H}_1 - H_0 \\ \overline{H}_2 - H_0 \end{bmatrix}.$$

Moreover, as above, if we target a specific variance-to-expectation ratio, conditionally a given trajectory of temperatures between dates 1 and t_{2100}, we obtain μ_H since, using (52):

$$\mu_H = \frac{\overline{\mathbb{V}ar}_0(H_{t_{2100}} | \underline{T_{AT,t_{2100}}})}{2\overline{\mathbb{E}}_0(H_{t_{2100}} | \underline{T_{AT,t_{2100}}})}. \tag{S.23}$$

S.D. TIME-SEPARABLE POWER UTILITY PREFERENCES

This appendix presents a modfied version of the model in which agents possess time-separable power utility preferences. Specifically, we utilize the following time-separable intertemporal

FIGURE S.1. Model calibration

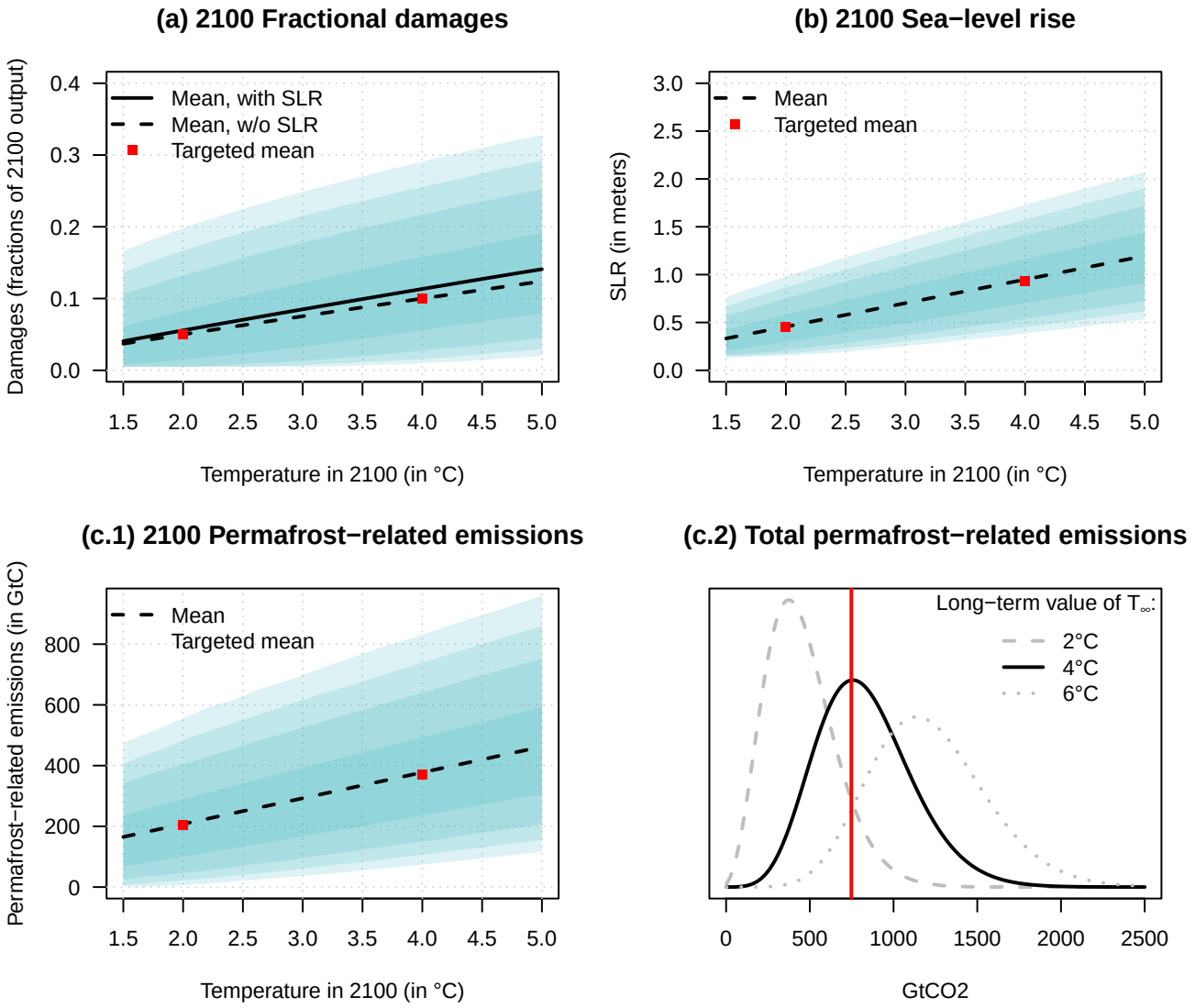

Notes: This figure illustrates the calibration approach by showing the fit of some moments pertaining to economic damages (D_t, eq. 13), sea level rise (H_t, eq. 8), and permafrost-related carbon releases (N_t, eq. 7). The damage specification involves 3 parameters (μ_D, $a^{(D)}$, and $b^{(D)}$), that are calibrated to match (D.i) the expectation of 2100 damages conditional on $T_{AT,h} = 2°C$, (D.ii) the expectation of 2100 damages conditional on $T_{AT,h} = 4°C$, and (D.iii) the 2100 standard deviation of damages conditional on $T_{AT,h} = 4°C$. The two red dots in Panel (a) correspond to (D.i) and (D.ii). The SLR specification involves 3 parameters (μ_H, $a^{(\Delta H)}$, and $b^{(\Delta H)}$), that are calibrated to match (SLR.i) the expectation of the 2100 sea level conditional on $T_{AT,h} = 2°C$, (SLR.ii) the expectation of the 2100 sea level conditional on $T_{AT,h} = 4°C$, and (SLR.iii) the 2100 standard deviation of sea level on $T_{AT,h} = 4°C$. The two red dots in Panel (b) correspond to (SLR.i) and (SLR.ii). The 4 parameters characterizing N_t's dynamics (μ_N, $a^{(N)}$, $b^{(N)}$, and κ_N) are calibrated to match the following conditional moments: (N.i) the expectation of the 2100 permafrost-related carbon release ($N_1 + \cdots + N_h$, period h corresponding to 2100) conditional on $T_{AT,h} = 2°C$, (N.ii) the same expectation, but conditional on $T_{AT,h} = 4°C$, (N.iii) the standard deviation of the 2100 permafrost-related carbon release conditional on $T_{AT,h} = 4°C$, and (N.iv) the expectation of total permafrost-related carbon release conditional on a long-run temperature value ($T_{AT,\infty} = 4°C$). The two red dots in Panel (c.1) correspond to (N.i) and (N.ii). The red vertical line in Panel (c.2) correspond to (N.iv). We refer to Appendix D the and the supplemental appendix for additional details on the calibration procedure.

value function, replacing (15):

$$U_t = \mathbb{E}_t\left(\sum_{k=0}^{\infty}\delta^k\frac{C_{t+k}^{1-\gamma}}{1-\gamma}\right). \tag{S.24}$$

S.D.1. **Consumption growth.** In that case, the Euler equation associated with capital is:

$$1 = \mathbb{E}_t\Big(\delta\left(\frac{C_{t+1}}{C_t}\right)^{-\gamma}\underbrace{\{(1-\Lambda_{t+1})A_{t+1}+1-dep\}}_{\approx\exp(\mu_{c,t+1}-\log\delta+\sigma_{c,t+1}\eta_{A,t+1})}\exp(-D_{t+1}-b_{SK}\Delta H_{t+1})\Big),$$

where $\mu_{c,t}$ and $\sigma_{c,t}$ are given in (19).

Hence, Δc_{t+1} must satisfy:

$$1 = \mathbb{E}_t\big(\exp[-\gamma\Delta c_{t+1}+\mu_{c,t+1}+\sigma_{c,t+1}\eta_{A,t+1}-D_{t+1}-b_{SK}\Delta H_{t+1}]\big).$$

An approximate solution for consumption growth is given by:

$$\Delta c_t = \mu_{c,0,t}+\mu_{c,1,t}'X_t := \frac{1}{\gamma}\left(\mu_{c,t}+\sigma_{c,t}\eta_{A,t}-D_t-b_{SK}\Delta H_t\right),$$

where $\mu_{c,t}$ and $\sigma_{c,t}$ are given in (19).

S.D.2. **Solving for the value function.** As in our baseline (Epstein-Zin) approach, agents establish the trajectory of mitigation rates $\{\mu_t\}_{t\geq 1}$ on the initial date. We maintain the parametric form given in (17) for these rates, with the future sequence of μ_t depending on $\{\theta_a,\theta_b\}$. On date $t=0$, agents thus determine $\{\theta_a,\theta_b\}$ to maximize the utility U_t given in (16). To perform this optimization, we must compute the utility, which we derive as follows:

$$\begin{aligned} U_t &= \frac{C_t^{1-\gamma}}{1-\gamma}\Big\{1+\sum_{k=1}^{\infty}\delta^k\exp((1-\gamma)(\mu_{c,0,t+1}+\cdots+\mu_{c,0,t+k}))\times \\ &\quad \exp\left(\psi_{0,t}^{(k)}(u_1,\ldots,u_k)+\psi_{1,t}^{(k)}(u_1,\ldots,u_k)'X_t\right)\Big\}, \end{aligned} \tag{S.25}$$

with $u_k = (1-\gamma)\mu_{c,1,t+k}$, and where functions $\psi_{0,t}^{(k)}$ and $\psi_{1,t}^{(k)}$ characterize the multi-horizon Laplace transform of X_t (see Proposition 2).

S.D.3. **Social Cost of Carbon.** Eq. (S.25) implies, in particular, that the SCC is given by:

$$\begin{aligned} SCC_t &= -\frac{\partial U_t}{\partial M_{AT,t}}\Big/\frac{\partial U_t}{\partial C_t} \\ &= \frac{C_t}{\gamma-1}\sum_{k=1}^{\infty}\delta^k\psi_{1,t,M_{AT}}^{(k)}(u_1,\ldots,u_k)\exp((1-\gamma)(\mu_{c,0,t+1}+\cdots+\mu_{c,0,t+k}))\times \\ &\quad \exp\left(\psi_{0,t}^{(k)}(u_1,\ldots,u_k)+\psi_{1,t}^{(k)}(u_1,\ldots,u_k)'X_t\right), \end{aligned}$$

where $\psi^{(k)}_{1,t,M_{AT}}(u_1,\ldots,u_k)$ denotes the component of vector $\psi^{(k)}_{1,t}(u_1,\ldots,u_k)$ associated with the carbon concentration $M_{AT,t}$.

Besides, in the present time-separable case, the SCC admits the decomposition (49), that is:

$$SCC_t = \sum_{h=1}^{\infty} \mathcal{B}_{t,h}\mathbb{E}_t(\mathcal{P}_{t,t+h}) + \sum_{h=1}^{\infty} \mathbb{C}ov_t(\mathcal{M}_{t,t+h}, \mathcal{P}_{t,t+h}),$$

where $\mathcal{P}_{t,t+h}$ represents the benefit in terms of consumption for date $t+h$, resulting from the decrease in $M_{AT,t}$ by one unit, that is, $\mathcal{P}_{t,t+h} = -\partial C_{t+h}/\partial M_{AT,t}$. It can be noted that our formulas allow to compute $\mathbb{E}_t(\mathcal{P}_{t,t+h})$ without resorting to simulations. Specifically, we have:

$$\begin{aligned}\mathbb{E}_t(\mathcal{P}_{t,t+h}) &= -\psi^{(h)}_{1,t,M_{AT}}(\mu_{c,1,t},\ldots,\mu_{c,1,t+h})\exp(\mu_{c,0,t}+\cdots+\mu_{c,0,t+h})\times \\ &\quad \exp\left[\psi^{(k)}_{0,t}(\mu_{c,1,t},\ldots,\mu_{c,1,t+h}) + \psi^{(k)}_{1,t}(\mu_{c,1,t},\ldots,\mu_{c,1,t+h})'X_t\right], \qquad \text{(S.26)}\end{aligned}$$

where $\psi^{(h)}_{0,t}$ and $\psi^{(h)}_{1,t}$ characterize the multi-horizon Laplace transform of X_t (see Proposition 2). Note that (S.26) is also valid in the Epstein-Zin context of our baseline model; this formula is used, in particular, when we compute SCC risk premiums (see Subsection 4.4).

Proof. We have

$$\begin{aligned}\mathbb{E}_t(\mathcal{P}_{t,t+h}) &= -\mathbb{E}_t\left(\frac{\partial}{\partial M_{AT,t}}C_{t+h}\right) = -C_t\frac{\partial}{\partial M_{AT,t}}\mathbb{E}_t(\exp(\Delta c_{t+1}+\cdots+\Delta c_{t+h})) \\ &= -\frac{\partial}{\partial M_{AT,t}}\Big(\exp\left[\mu_{c,0,t}+\cdots+\mu_{c,0,t+h}+\psi^{(h)}_t(\mu_{c,1,t},\ldots,\mu_{c,1,t+h})\right]\Big) \\ &= -\frac{\partial}{\partial M_{AT,t}}\Big(\exp(\mu_{c,0,t}+\cdots+\mu_{c,0,t+h})\times \\ &\quad \exp\left[\psi^{(h)}_{0,t}(\mu_{c,1,t},\ldots,\mu_{c,1,t+h}) + \psi^{(h)}_{1,t}(\mu_{c,1,t},\ldots,\mu_{c,1,t+h})'X_t\right]\Big),\end{aligned}$$

which gives (S.26). □

S.D.4. **Stochastic discount factor and pricing.** The stochastic discount factor is given by $\mathcal{M}_{t,t+1} = \delta\exp(-\gamma\Delta c_{t+1})$. Using the same notations as in Proposition 4, we have:

$$\mathcal{M}_{t,t+1} = \exp[-(\mu_{r,0,t+1}+\mu'_{r,1,t+1}X_t) + \Pi'_{t+1}X_{t+1} \underbrace{-\alpha_t(\Pi_{t+1}) - \beta_t(\Pi_{t+1})'X_t}_{=-\psi_t(\Pi_{t+1}),\text{ see eq. (21)}}], \qquad \text{(S.27)}$$

where

$$\begin{cases} \Pi_{t+1} &= -\gamma\mu_{c,1,t+1} \\ \mu_{r,0,t+1} &= -\log\delta + \gamma\mu_{c,0,t+1} - \alpha_t(\Pi_{t+1}) \\ \mu_{r,1,t+1} &= -\beta_t(\Pi_{t+1}). \end{cases} \qquad \text{(S.28)}$$

Using these notations, all the pricing formulas presented in Appendix S.B remain valid.

S.D.5. **Model outputs.** Panels B of Tables 5, S.1, and S.2 respectively show the SCCs, the temperature risk premiums, and the long-term rates (of maturity 2100) based on the power-utility version of the model. (In each table, Panel A shows the Epstein-Zin-based results.)

Table 5 shows that SCCs estimates are much smaller than with Epstein-Zin preferences for risk aversion parameters that are substantially above one. This essentially comes from the fact that, in the CRRA case, discount rates increase with risk aversion (see Panel B of Table S.2), which reduces the net present value of the future benefits associated with reductions of carbon in the atmosphere; this echoes the results of Daniel, Litterman, and Wagner (2019).

S.E. On the optimality of the mitigation process

To get instant results, the representative agent of our model is not allowed to re-optimize the mitigation rate μ_t on each date. Instead, she decides the mitigation rate path (μ_t) only once and for all on the initial date, and further commits to that parametric path. Formally, she solves (16) where the utility u is given in Proposition 3, and where the parametric form is specified in (17).

This parametric time function is inspired by the usual forms of emission control rates obtained in standard IAMs (see, e.g., Cai and Lontzek, 2019, Figure 2.C). Panel (a) of Figure 11 displays our model-implied emission control rate μ_t (black solid line). For the sake of comparison, the figure also shows the emission control rate prevailing in the 2016 version of the DICE model (Nordhaus, 2017) (grey dashed line).

Our approach does not allow abatement to respond to jumps in damages or emissions. Arguably, such a response would mitigate some of the risk under consideration; moreover, it may introduce a policy component to risk, which is missing here. In order to assess these potential shortcomings, we proceed to two exercises:

(i) We replace the parametric function (17) (or 16) with a complete sequence of μ_t's that the agents determine on date 0. That is, we replace (16) with:

$$\{\mu_{1,opt},\dots,\mu_{k,opt},\dots\} := \underset{\mu_1,\dots,\mu_k,\dots}{\operatorname{argmax}}\ u_0[\mu_1,\dots,\mu_k,\dots]. \tag{S.29}$$

(ii) We look at how agents would modify the future sequence of μ_t's if they were given the chance to, for dates $t > 0$. (On each instance, they think that is the last time they can do so.) That is, we compute a sequence of pairs $\{\theta_{a,opt},\theta_{b,opt}\}_t$ defined by:

$$\{\theta_{a,opt},\theta_{b,opt}\}_t := \underset{\theta_a,\theta_b}{\operatorname{argmax}}\ u_t[\mu_{t+1}(\theta_a,\theta_b),\dots,\mu_{t+k}(\theta_a,\theta_b),\dots]. \tag{S.30}$$

Note that the solution to the previous maximization problem depends on the state vector prevailing at date t (that is X_t). Our analysis considers three different cases:

FIGURE S.2. Mitigation rate

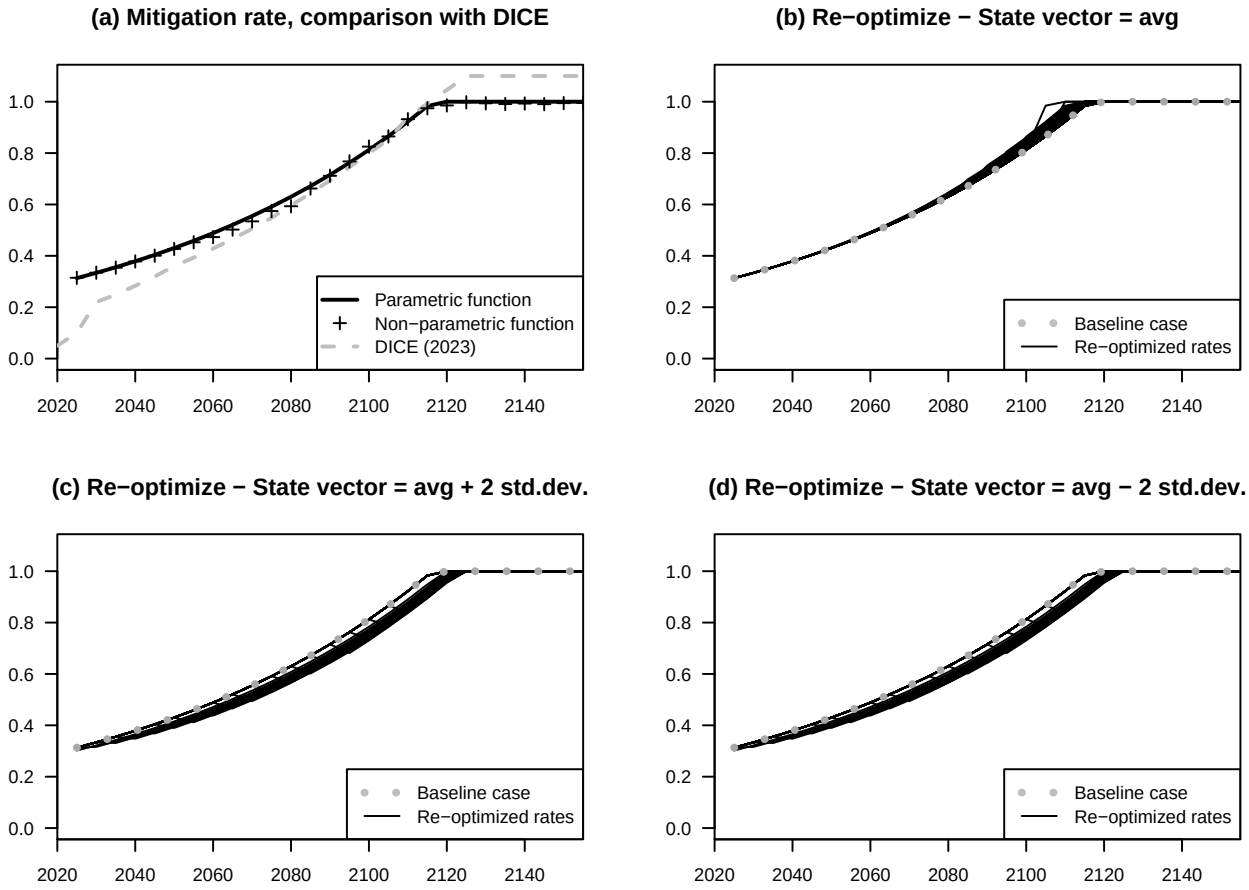

Notes: The grey dashed line in Panel (a) represents the mitigation rate of the 2023 version of the DICE (Barrage and Nordhaus, 2023). In Panel (a), the black solid line is our baseline sequence of mitigation rates, resulting from problem (16). The crosses are the solutions to the same type of problem, but without using a parametric formulation for the μ_t's (see problem S.29). Panels (b) to (d) display the sequences of μ_t resulting from re-optimizations taking place at later periods: for each date t, we determine the pair $\{\theta_{a,opt}, \theta_{b,opt}\}_t$ that maximizes $u_t[\mu_{t+1}(\theta_a, \theta_b), \dots, \mu_{t+k}(\theta_a, \theta_b), \dots]$ (see problem S.30). These optimizations depend on the value of the state vector on date t (X_t). We consider three cases: X_t is set at $\mathbb{E}_0(X_t)$ (Panel (b)); X_t is set at $\mathbb{E}_0(X_t) + 2SD_0(X_t)$ (Panel (c)); X_t is set at $\mathbb{E}_0(X_t) - 2SD_0(X_t)$ (Panel (d)), where $SD_0(X_t)$ denotes the vector of standard deviations of X_t, conditional on date 0.

$X_t = \mathbb{E}_0(X_t)$, $X_t = \mathbb{E}_0(X_t) + 2SD_0(X_t)$, and $X_t = \mathbb{E}_0(X_t) - 2SD_0(X_t)$, where $SD_0(X_t)$ denotes the vector of standard deviations of X_t, conditional on date 0.

The results of these two exercises are displayed on Figure S.2:

(i) Panel (a) of Figure S.2 compares the baseline case (the solution to problem 16) with the "non-parametric" one (problem S.29). The two trajectories are close to one another.

(ii) Each Panel (b) to (d) shows the results of problem (S.30), for $t \in \{1, \dots, 40\}$ (i.e., 200 years). That is, each panel reports 40 trajectories (black lines) of mitigation rates. (Trajectory t is $\{\mu_{t+1}, \mu_{t+2}, \dots\}$). The three panels differ in the value of the initial state

value: X_t is set at $\mathbb{E}_0(X_t)$ in Panel (b); X_t is set at $\mathbb{E}_0(X_t) + 2SD_0(X_t)$ in Panel (c); X_t is set at $\mathbb{E}_0(X_t) - 2SD_0(X_t)$ in Panel (d), where $SD_0(X_t)$ denotes the vector of standard deviations of X_t, conditional on date 0.

The results suggest that mitigation rate trajectories are not too sensitive to the possibility of re-optimization over time.

Additionally, we have verified that our asset pricing implications are robust to our modeling of the mitigation path. Specifically, for each date (t), we compared the SCCs and the 50-year temperature risk premiums derived from the alternative models underlying Panels (a) to (d) with those from our baseline approach (where the μ_t trajectory is parametric and determined ex-ante, with no updates). It appears that SCCs remain virtually unchanged, and changes in temperature risk premiums are lower than 1%.

S.F. Additional results

S.F.1. **SCC risk premiums versus temperature risk premiums.** The temperature risk premium is the difference between the risk-adjusted temperature and its physical counterpart, for a given horizon, see Subsection 4.4, and more particularly (45). Table S.1 documents the sensitivity of the temperature risk premium to different model ingredients.

We define the SCC risk premium as the difference between the SCC and the sum of discounted expected consumption benefits associated with the removal of one ton of CO_2 from the atmosphere. Using the notations of (49), it is given by

$$SCC_t^{RP} = SCC_t - \sum_{h=1}^{\infty} \mathcal{B}_{t,h}\mathbb{E}_t(\mathcal{P}_{t,t+h}), \tag{S.31}$$

where $\mathcal{P}_{t,t+h}$ represents such benefits for date $t+h$, that is, $\mathcal{P}_{t,t+h} = -\partial C_{t+h}/\partial M_{AT,t}$, and where $\mathcal{B}_{t,h}$ is the date-t price of a zero-coupon bond of maturity h. Note that $\mathbb{E}_t(\mathcal{P}_{t,t+h})$ is given by (S.26) in both the Epstein-Zin and time-separable CRRA cases.

Figure S.3 shows how the SCC risk premiums and the 2100 temperature risk premiums jointly depend on the volatility of exogenous technological progress (σ_A, black line) or the scale of damages (in grey). The SCC risk premium is measured as the difference between the SCC and the sum of discounted expected benefits associated with the removal of one ton of CO_2 from the atmosphere, expressed as a fraction of the SCC (as in Daniel et al., 2019).[4] Panel (a) corresponds to our baseline framework, with Epstein-Zin preferences; Panels (b) and (c) correspond to CRRA versions of the model, with two different risk aversion parameters. Start with the effect of σ_A, the volatility of exogenous technological progress (black line). Both the SCC risk premium and the temperature risk premium decrease when σ_A increases, under the

[4]The date-t expectation of the benefit for date $t+h$, namely $\mathbb{E}_t(\mathcal{P}_{t,t+h})$ of (49), can be calculated by evaluating the multi-horizon Laplace transform $\psi_t^{(h)}$ at $(\mu_{c,1,t+1}, \ldots, \mu_{c,1,t+h})$ (see Supplemental Appendix S.D.3).

effects of the *scaling channel* and of the *capital accumulation channel*, respectively. Consistently with Dietz et al. (2018) and Lemoine (2021), in the CRRA case (Panels b and c), the SCC risk premium is positive for $\sigma_A = 0$, and it turns negative for higher values of σ_A. Turn to the effect of the scale of damages on the two types of risk premiums (grey lines). The relative importance of risk premiums in the SCC maintains the same order of magnitude when the scale of damages varies; but since the SCC positively depends on the scale of damages, the SCC risk premium also increases in absolute value. The temperature risk premium also positively depends on the scale of damages, consistently with the *damage channel* defined above.

TABLE S.1. 2100 Temperature risk premium

A. Epstein-Zin preferences						
Specification	$\gamma = 7$		$\gamma = 2$		$\gamma = 10$	
Baseline	**0.092**		**0.030**		**0.162**	
Large rate of pref. for present ($-\log(\delta)/\Delta t = 1.5\%$)	0.057	*−0.035°C*	0.026	*−0.004°C*	0.095	*−0.067°C*
Small rate of pref. for present ($-\log(\delta)/\Delta t = 0.5\%$)	0.233	*+0.141°C*	0.047	*+0.017°C*	0.488	*+0.326°C*
Large climate sensitivity ($\nu = 4$)	0.157	*+0.065°C*	0.046	*+0.016°C*	0.280	*+0.118°C*
Small climate sensitivity ($\nu = 2$)	0.013	*−0.079°C*	0.007	*−0.023°C*	0.025	*−0.137°C*
Deterministic model	0.023	*−0.069°C*	0.023	*−0.007°C*	0.023	*−0.139°C*
No exog. techno. uncertainty ($\sigma_A = 0$)	0.119	*+0.027°C*	0.038	*+0.009°C*	0.197	*+0.034°C*
No uncert. on damage specif. ($\mu_D = 0$)	0.065	*−0.027°C*	0.028	*−0.001°C*	0.091	*−0.071°C*
No uncert. on permafrost specif. ($\mu_N = 0$)	0.012	*−0.080°C*	0.017	*−0.013°C*	0.014	*−0.148°C*
No uncert. on sea-level specif. ($\mu_H = 0$)	0.092	*−0.000°C*	0.030	*−0.000°C*	0.162	*−0.000°C*
No uncert. on temperature specif. ($\mu_T = 0$)	0.075	*−0.017°C*	0.027	*−0.002°C*	0.131	*−0.031°C*
Small damages (twice lower)	0.020	*−0.072°C*	0.019	*−0.011°C*	0.025	*−0.137°C*
No permaf. releases ($a^{(N)} = b^{(N)} = 0$)	−0.020	*−0.112°C*	−0.008	*−0.038°C*	−0.023	*−0.185°C*
No sea-level-specific damages ($a^{(H)} = b^{(H)} = 0$)	0.078	*−0.014°C*	0.027	*−0.003°C*	0.140	*−0.023°C*
B. Time-separable CRRA preferences						
Specification	$\gamma = 1.5$		$\gamma = 1.001$		$\gamma = 2$	
Baseline	**0.016**		**0.021**		**0.008**	
Large rate of pref. for present ($-\log(\delta)/\Delta t = 1.5\%$)	0.017	*+0.001°C*	0.022	*+0.000°C*	0.009	*+0.001°C*
Small rate of pref. for present ($-\log(\delta)/\Delta t = 0.5\%$)	0.016	*−0.000°C*	0.021	*−0.000°C*	0.008	*−0.001°C*
Large climate sensitivity ($\nu = 4$)	0.026	*+0.010°C*	0.031	*+0.009°C*	0.019	*+0.011°C*
Small climate sensitivity ($\nu = 2$)	0.001	*−0.015°C*	0.006	*−0.015°C*	−0.007	*−0.015°C*
Deterministic model	0.023	*+0.007°C*	0.024	*+0.002°C*	0.024	*+0.015°C*
No exog. techno. uncertainty ($\sigma_A = 0$)	0.029	*+0.013°C*	0.027	*+0.006°C*	0.031	*+0.023°C*
No uncert. on damage specif. ($\mu_D = 0$)	0.015	*−0.001°C*	0.021	*−0.000°C*	0.007	*−0.001°C*
No uncert. on permafrost specif. ($\mu_N = 0$)	0.011	*−0.005°C*	0.018	*−0.004°C*	0.001	*−0.008°C*
No uncert. on sea-level specif. ($\mu_H = 0$)	0.016	*−0.000°C*	0.021	*−0.000°C*	0.008	*−0.000°C*
No uncert. on temperature specif. ($\mu_T = 0$)	0.016	*−0.000°C*	0.021	*−0.000°C*	0.008	*−0.000°C*
Small damages (twice lower)	0.010	*−0.006°C*	0.018	*−0.003°C*	−0.002	*−0.010°C*
No permaf. releases ($a^{(N)} = b^{(N)} = 0$)	−0.013	*−0.029°C*	−0.006	*−0.027°C*	−0.023	*−0.031°C*
No sea-level-specific damages ($a^{(H)} = b^{(H)} = 0$)	0.015	*−0.001°C*	0.020	*−0.001°C*	0.006	*−0.002°C*

Notes: This table documents the sensitivity of the 2100 temperature risk premium to several modeling ingredients. The baseline value of the climate sensitivity (ν) is 3.25 (eq. 1), and the baseline value of the rate of pure preference for present is $-\log(\delta)/\Delta t = 1\%$ The deterministic model is a model where we remove all sources of uncertainty ($\mu_D = \mu_N = \mu_T = \mu_H = \sigma_A = 0$). Values in italics indicate changes from the baseline case. In the "Small damages" scenario, both $\lambda_{D,t}$ (eq. 13) and $\lambda_{H,t}$ (eq. 8) are divided by 2. "bps" stands for basis points.

FIGURE S.3. Social Cost of Carbon and temperature risk premiums

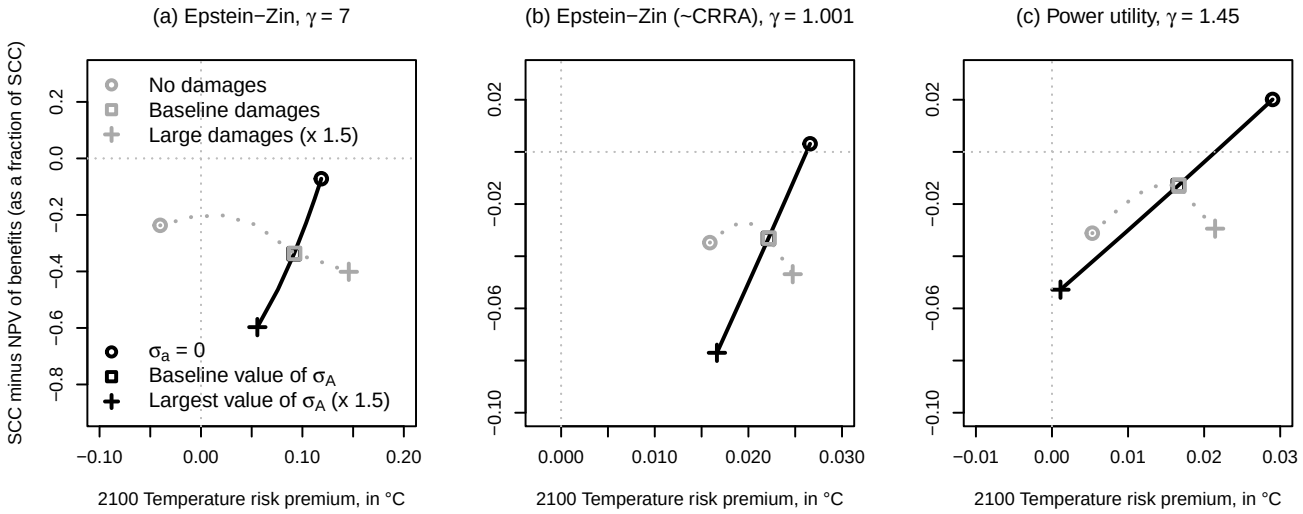

Notes: This figure shows the relationship between SCC and temperature risk premiums when varying the volatility of exogenous technological progress (black line) or the scale of damages (in grey). The x-axis coordinates are 2100 temperature risk premiums—the difference between the risk-adjusted and the physical expectation of temperature. The y-axis coordinate is the difference between the SCC and the sum discounted expected benefits associated with the removal of one ton of CO_2 from the atmosphere, expressed as a fraction of the SCC. Since we consider a unit intertemporal elasticity of substitution in the Epstein-Zin context, Panel (B), where $\gamma \approx 1$, corresponds to a situation where the Epstein-Zin and CRRA-based preferences coincide. The values of σ_A (see eq. 10) go from 0 to 1.5 times its baseline value (see Table 1). For damages, we jointly rescale $a^{(D)}$, $b^{(D)}$, μ_D, and b_{SK}.

While Figure S.3 focuses on the 2100 horizon, there exists a whole-term structure of temperature risk premiums. This is shown in Figure S.4, which compares the term structure based on the present model to those resulting from alternative approaches, namely Lemoine (2021) and Bansal et al. (2019).

S.F.2. **Long-term rates: sensitivity analysis.** Table S.2 documents the sensitivity of the long-term real rate to key modeling ingredients. The long-term rate refers to the risk-free rate associated with a bond maturing in 2100.

S.F.3. **Equity and bonds whose issuer is exposed to climate risk.** This subsection shows how the model can be combined with the Black-Scholes-Merton framework (Black and Scholes, 1973; Merton, 1974) to investigate the influence of climate risks on bond and equity prices.

At the heart of the model stands the specification of the process followed by the value of a firm's asset ($\mathcal{A}_t$). The firm issues two types of financial instruments: equity and debt. Equity shares do not entitle the holders to receive dividends. Debt, on the other hand, takes the form of a zero-coupon bond that promises a payment of $\overline{\mathcal{A}}$ at a specified time ($t + h$, say). If the firm's asset value at time $t + h$ is greater than $\overline{\mathcal{A}}$, bondholders receive this amount, and the remaining asset value goes to shareholders. However, if the asset value falls short of the

FIGURE S.4. Comparison of temperature risk premiums

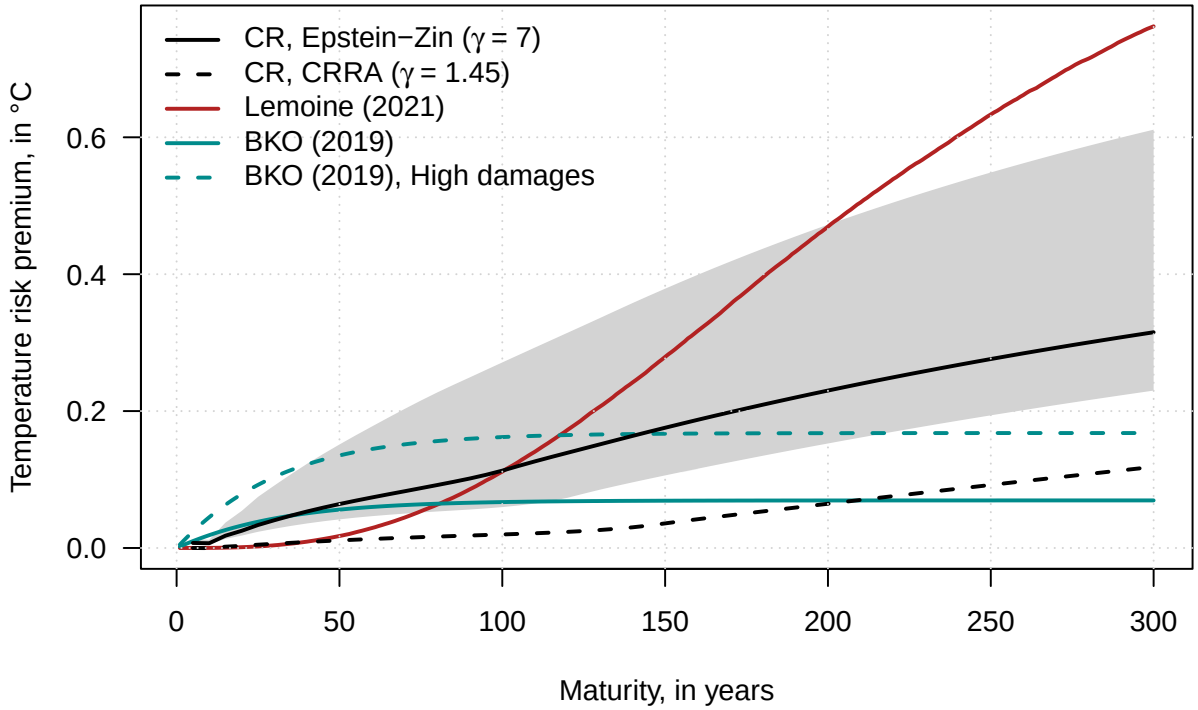

Notes: This figure displays term structures of temperature risk premiums. This risk premium is defined in (44); it reflects agents' aversion to the randomness of future temperature. The two 'CR' curves are based on the present framework, using Epstein-Zin preferences for the solid line (with $\gamma = 7$), and time-separable CRRA preferences for the dashed line (with $\gamma = 1.45$, as in Lemoine, 2021). The grey shaded area is delineated by term structures stemming from two alternative versions of the model where the rate of pure preference for the present is 0.5% (upper bound of the area) or 1.5% (lower bound of the area). The red curve is based on the model proposed by Lemoine (2021), considering a simplified distribution for the climate sensitivity and the damage function. 'BKO' refers to Bansal et al. (2019). For the latter, we consider two damage specifications, the baseline one (solid line) and a second one (dashed line) where damages are twice larger.

promised payment, the firm defaults, resulting in the lenders receiving a payment equal to the asset value, while shareholders receive no payment. Hence, in this model, the equity of the firm is modeled as a call option on its assets.

We assume that:

$$\log \mathcal{A}_t = \log \mathcal{A}_{t-1} + r_{A,t}, \quad \text{with} \quad r_{A,t} = \mu_{A,0,t} + \mu'_{A,1} X_t, \tag{S.32}$$

where $\mu_{A,0,t}$ is deterministic. Notice that $\mu_{A,0,t}$ cannot be chosen independently from $\mu_{A,1}$ because the firm's value has to satisfy the Euler equation.[5]

[5]We must have, for any $h > 0$: $\mathbb{E}_t(\mathcal{M}_{t,t+h} \exp(r_{A,t+1} + \cdots + r_{A,t+h})) = 1$. In other words, once we specify $\mu_{A,1}$, the sequence of $\mu_{A,0,t}$ is given. Take a given $\mu_{A,1}$. Define $\widetilde{A}_t$ such that $\log \widetilde{A}_t = \log \widetilde{A}_{t-1} + \mu'_{A,1} X_t$, and determine $\widetilde{\mu}_A$ such that $\log(\widetilde{A}_t) = \widetilde{\mu}'_A X_t$. Assume you have already computed $\{\mu_{A,0,t+1}, \ldots, \mu_{A,0,t+h-1}\}$. Since $\mathbb{E}_t(\mathcal{M}_{t,t+h} \widetilde{A}_{t+h}) = \varphi_t^{(h)}(\widetilde{\mu}_A)$, and since the Euler equation rewrites $\exp(\mu_{A,0,t+1} + \cdots + \mu_{A,0,t+h}) \mathbb{E}_t(\mathcal{M}_{t,t+h} \widetilde{A}_{t+h}) = 1$, it comes that $\mu_{A,0,t+h} = -\log(\varphi_t^{(h)}(\widetilde{\mu}_A)) - \mu_{A,0,t+h-1} - \cdots - \mu_{A,0,t+1}$.

TABLE S.2. Long-term interest rate (maturity: 2100)

A. Epstein-Zin preferences						
Specification	$\gamma = 7$		$\gamma = 2$		$\gamma = 10$	
Baseline	**2.25**		**2.41**		**2.13**	
Large rate of pref. for present ($-\log(\delta)/\Delta t = 1.5\%$)	2.27	*+2 bps*	2.43	*+2 bps*	2.15	*+3 bps*
Small rate of pref. for present ($-\log(\delta)/\Delta t = 0.5\%$)	2.17	*−8 bps*	2.34	*−7 bps*	2.02	*−10 bps*
Large climate sensitivity ($\nu = 4$)	2.20	*−5 bps*	2.38	*−3 bps*	2.06	*−7 bps*
Small climate sensitivity ($\nu = 2$)	2.35	*+10 bps*	2.48	*+7 bps*	2.25	*+13 bps*
Deterministic model	2.46	*+20 bps*	2.46	*+5 bps*	2.46	*+33 bps*
No exog. techno. uncertainty ($\sigma_A = 0$)	2.36	*+11 bps*	2.44	*+3 bps*	2.29	*+16 bps*
No uncert. on damage specif. ($\mu_D = 0$)	2.34	*+9 bps*	2.43	*+2 bps*	2.29	*+16 bps*
No uncert. on permafrost specif. ($\mu_N = 0$)	2.26	*+0 bps*	2.41	*+0 bps*	2.14	*+1 bps*
No uncert. on sea-level specif. ($\mu_H = 0$)	2.25	*+0 bps*	2.41	*+0 bps*	2.13	*+0 bps*
No uncert. on temperature specif. ($\mu_T = 0$)	2.25	*+0 bps*	2.41	*+0 bps*	2.13	*+0 bps*
Small damages (twice lower)	2.41	*+15 bps*	2.50	*+9 bps*	2.34	*+22 bps*
No permaf. releases ($a^{(N)} = b^{(N)} = 0$)	2.29	*+4 bps*	2.44	*+3 bps*	2.18	*+6 bps*
No sea-level-specific damages ($a^{(H)} = b^{(H)} = 0$)	2.27	*+2 bps*	2.43	*+2 bps*	2.15	*+2 bps*
B. Time-separable CRRA preferences						
Specification	$\gamma = 1.5$		$\gamma = 1.001$		$\gamma = 2$	
Baseline	**3.17**		**2.45**		**3.88**	
Large rate of pref. for present ($-\log(\delta)/\Delta t = 1.5\%$)	3.17	*+1 bps*	2.46	*+1 bps*	3.88	*+1 bps*
Small rate of pref. for present ($-\log(\delta)/\Delta t = 0.5\%$)	3.16	*−1 bps*	2.44	*−1 bps*	3.87	*−1 bps*
Large climate sensitivity ($\nu = 4$)	3.13	*−4 bps*	2.42	*−3 bps*	3.82	*−5 bps*
Small climate sensitivity ($\nu = 2$)	3.25	*+9 bps*	2.51	*+6 bps*	3.99	*+12 bps*
Deterministic model	3.20	*+4 bps*	2.47	*+2 bps*	3.94	*+6 bps*
No exog. techno. uncertainty ($\sigma_A = 0$)	3.19	*+2 bps*	2.46	*+1 bps*	3.91	*+3 bps*
No uncert. on damage specif. ($\mu_D = 0$)	3.18	*+2 bps*	2.46	*+1 bps*	3.90	*+3 bps*
No uncert. on permafrost specif. ($\mu_N = 0$)	3.17	*+0 bps*	2.45	*+0 bps*	3.88	*+0 bps*
No uncert. on sea-level specif. ($\mu_H = 0$)	3.17	*+0 bps*	2.45	*+0 bps*	3.88	*+0 bps*
No uncert. on temperature specif. ($\mu_T = 0$)	3.17	*+0 bps*	2.45	*+0 bps*	3.88	*+0 bps*
Small damages (twice lower)	3.28	*+12 bps*	2.53	*+8 bps*	4.03	*+16 bps*
No permaf. releases ($a^{(N)} = b^{(N)} = 0$)	3.20	*+3 bps*	2.47	*+2 bps*	3.92	*+4 bps*
No sea-level-specific damages ($a^{(H)} = b^{(H)} = 0$)	3.19	*+2 bps*	2.47	*+2 bps*	3.91	*+3 bps*

Notes: This table documents the sensitivity of the real rate of maturity 2100 to several modeling ingredients. The baseline value of the climate sensitivity (ν) is 3.25 (eq. 1), and the baseline value of the rate of pure preference for present is $-\log(\delta)/\Delta t = 1\%$ The deterministic model is a model where we remove all sources of uncertainty ($\mu_D = \mu_N = \mu_T = \mu_H = \sigma_A = 0$). Values in italics indicate changes from the baseline case. In the "Small damages" scenario, both $\lambda_{D,t}$ (eq. 13) and $\lambda_{H,t}$ (eq. 8) are divided by 2. "bps" stands for basis points.

This specification allows, for example, temperature and sea level to affect the growth rate of $\mathcal{A}_t$; this is done by setting the appropriate entries of vector $\mu_{A,1}$ to non-zero values. As in the case of the price index (eq. 42), $\log \mathcal{A}_t$ can be included among the state vector's components, such that $\log \mathcal{A}_t = \mu_A' X_t$ (which defines the selection vector μ_A).

The date-t price of a zero-coupon bond of residual maturity h then is:

$$\begin{aligned} \mathcal{B}^*_{t,h} &:= \mathbb{E}_t\left(\mathcal{M}_{t,t+h}\left\{\mathbb{1}_{\{\mathcal{A}_{t+h}>\overline{\mathcal{A}}\}} + \frac{\mathcal{A}_{t+h}}{\overline{\mathcal{A}}}\mathbb{1}_{\{\log(\mathcal{A}_{t+h})\leq\log(\overline{\mathcal{A}})\}}\right\}\right) \\ &= \hat{\varphi}_t^{(h)}\left(0, -\mu_A, -\log(\overline{\mathcal{A}})\right) + \frac{1}{\overline{\mathcal{A}}}\bar{\varphi}_t^{(h)}\left(\mu_A, \mu_A, \log(\overline{\mathcal{A}})\right), \end{aligned}$$

where functions $\hat{\varphi}_t^{(h)}$ and $\bar{\varphi}_t^{(h)}$ are defined through (38) and (39), respectively.

The value of the firm's equity can then be expressed as the value of a call option on the firm's assets:

$$\begin{aligned} Equity_t &:= \mathbb{E}_t\left(\mathcal{M}_{t,t+h}\left\{(\mathcal{A}_{t+h}-\overline{\mathcal{A}})\mathbb{1}_{\{\mathcal{A}_{t+h}>\overline{\mathcal{A}}\}}\right\}\right) \\ &= \bar{\varphi}_t^{(h)}\left(\mu_A, -\mu_A, -\log(\overline{\mathcal{A}})\right) - \overline{\mathcal{A}}\hat{\varphi}_t^{(h)}\left(0, -\mu_A, -\log(\overline{\mathcal{A}})\right). \end{aligned}$$

Notice that the present modeling framework is richer than the original Black-Scholes-Merton framework as it features stochastic interest rates—the risk-free bond price formula of Subsection 4.3 are still valid—and the firm value may be affected by various sources of uncertainty.

FIGURE S.5. Merton model

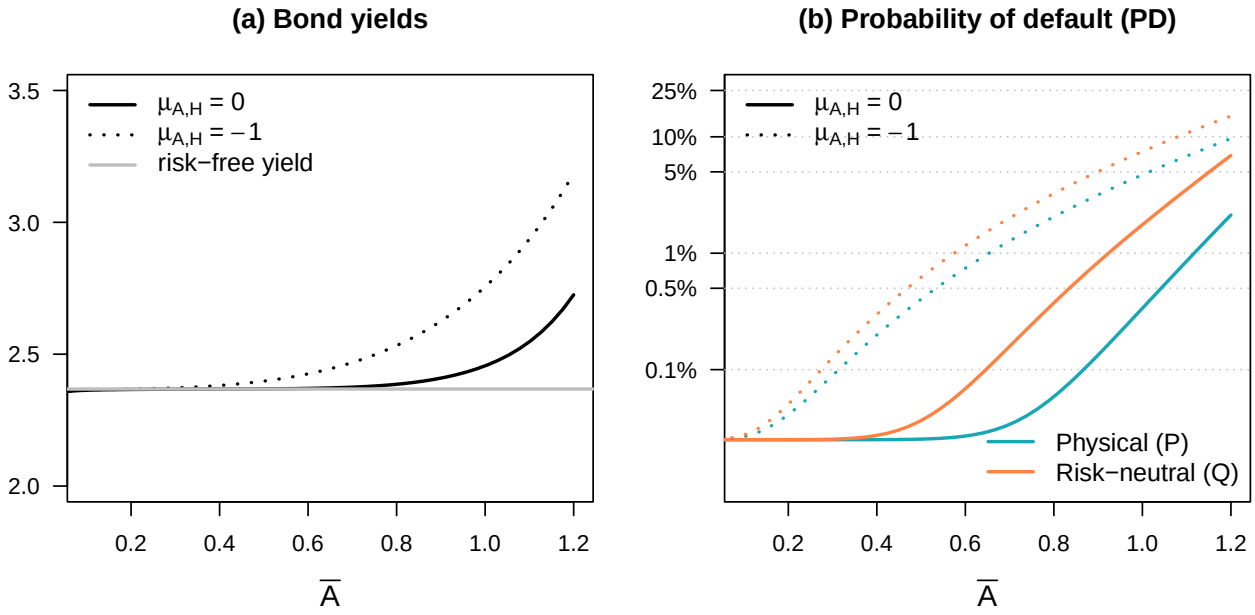

Notes: This figure shows outputs of the Black-Scholes-Merton model described in Subsection S.F.3. The x-axes correspond to varying values of $\overline{\mathcal{A}}$, which measures the firm's indebtedness. We consider two types of firms, represented by solid lines and dotted lines; the second type is more exposed to climate-related damages. Panel (a) displays bond yields; Panel (b) shows risk-neutral and physical probabilities of defaults (PDs).

In our numerical example, we consider two firms: a benchmark firm and a "coastal" one, that is particularly exposed to SLR risk. The growth rate of the asset value of the latter is characterized by $\mu_{A,1}' X_t = \chi \Delta c_t$, where χ is sometimes referred to as the leverage parameter in the literature.[6] The second firm exhibits a heightened vulnerability to sea level changes; it is such that $\mu_{A,1}' X_t = \chi \Delta c_t - H_t$. In other words, an unexpected 0.1-meter rise in sea level means that the company's value growth rate is reduced by 10 percentage points (or 2% annually, as

[6] We set this parameter to 2.5, in line with the values found in Abel (1999), Collin-Dufresne et al. (2016) and Seo and Wachter (2018) (2.74, 2.5 and 2.6, respectively).

one period is five years). In that context, the asset value of the second firm is expected to grow faster as investors demand a higher return to compensate for their greater risk-taking. For this specification, the expected annual growth rate of the second firm's asset value is 6 basis points higher than for the first firm.

Let us now turn to bond pricing. In our example, we consider a single maturity, of 20 years. Panel (a) of Figure S.5 displays the yields-to-maturity of the bonds issued by the two types of firms, as a function of firms' indebtedness ($\overline{\mathcal{A}}$). The "coastal" firm faces higher funding costs, reflecting higher probabilities of default (PDs); these PDs are plotted in Panel (b). This plot distinguishes risk-neutral and physical PDs. As is usual in credit-risk models, risk-neutral PDs are higher than physical ones, which reflects the fact that defaults tend to take place in bad states of the world (see, e.g., D'Amato and Remolona, 2003).

REFERENCES

Abel, A. B. (1999). Risk Premia and Term Premia in General Equilibrium. *Journal of Monetary Economics 43*(1), 3–33.

Bansal, R., D. Kiku, and M. Ochoa (2019). Climate Change Risk. Technical report, Fuqua Sch. Bus., Duke Univ., Durham, NC.

Barrage, L. and W. D. Nordhaus (2023). Policies, Projections, and the Social Cost of Carbon: Results from the DICE-2023 Model. Working Paper 31112, National Bureau of Economic Research.

Black, F. and M. S. Scholes (1973). The Pricing of Options and Corporate Liabilities. *Journal of Political Economy 81*(3), 637–54.

Cai, Y. and T. S. Lontzek (2019). The Social Cost of Carbon with Economic and Climate Risks. *Journal of Political Economy 127*(6), 2684–2734.

Collin-Dufresne, P., M. Johannes, and L. A. Lochstoer (2016). Parameter Learning in General Equilibrium: The Asset Pricing Implications. *The American Economic Review 106*(3), 664–698.

D'Amato, J. and E. M. Remolona (2003). The Credit Spread Puzzle. *BIS Quarterly Review*.

Daniel, K. D., R. B. Litterman, and G. Wagner (2019). Declining CO_2 Price Paths. *Proceedings of the National Academy of Sciences 116*(42), 20886–20891.

Dietz, S., C. Gollier, and L. Kessler (2018). The Climate Beta. *Journal of Environmental Economics and Management 87*(C), 258–274.

Lemoine, D. (2021). The Climate Risk Premium: How Uncertainty Affects the Social Cost of Carbon. *Journal of the Association of Environmental and Resource Economists 8*(1), 27–57.

Merton, R. C. (1974). On the Pricing of Corporate Debt: The Risk Structure of Interest Rates. *Journal of Finance 29*(2), 449–70.

Nordhaus, W. D. (2017). Revisiting the Social Cost of Carbon. *Proceedings of the National Academy of Sciences 114*(7), 1518–1523.

Piazzesi, M. and M. Schneider (2007). Equilibrium Yield Curves. In *NBER Macroeconomics Annual 2006, Volume 21*, NBER Chapters, pp. 389–472. National Bureau of Economic Research, Inc.

Seo, S. B. and J. A. Wachter (2018). Do Rare Events Explain CDX Tranche Spreads? *Journal of Finance 73*, 2343–2383.